PARADIM
AN NSF MATERIALS INNOVATION PLATFORM

Lecture #2—
Nuts and Bolts of Oxide MBE: Growth Conditions, Sources, and Crucibles

Darrell G. Schlom

Nuts and Bolts of Oxide MBE

How to grow your favorite oxide by MBE?

- Lecture #2—*Growth Conditions, Sources, and Crucibles*
- Lecture #3—*Composition Control and Calibration*
- Lecture #4—*Epitaxy, Substrates, and Crystal Growth*

PARADIM

NSF

Nuts and Bolts of Oxide MBE

- Mean Free Path (maximum P_{O_2})
- Minimum P_{O_2}, need for P_{O_3}
- Optimal T_{sub}
- MBE System
- MBE Sources
- Crucibles

PARADIM

NSF

Maximum O_2 Pressure for MBE

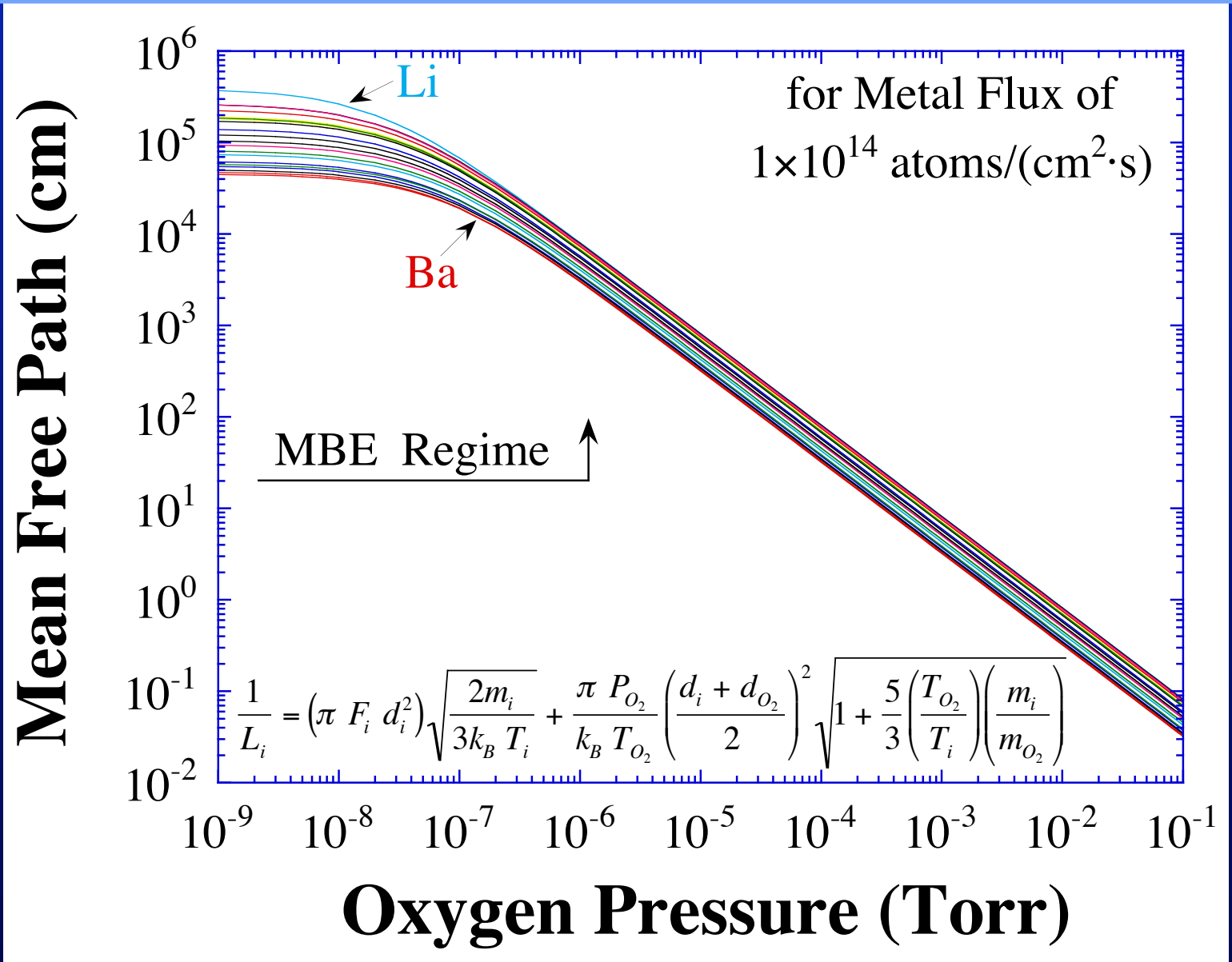

D.G. Schlom and J.S. Harris, Jr., in *Molecular Beam Epitaxy: Applications to Key Materials*, edited by R.F.C. Farrow (Noyes, Park Ridge, 1995), pp. 505-622.

O_2 Needed to Oxidize Constituents

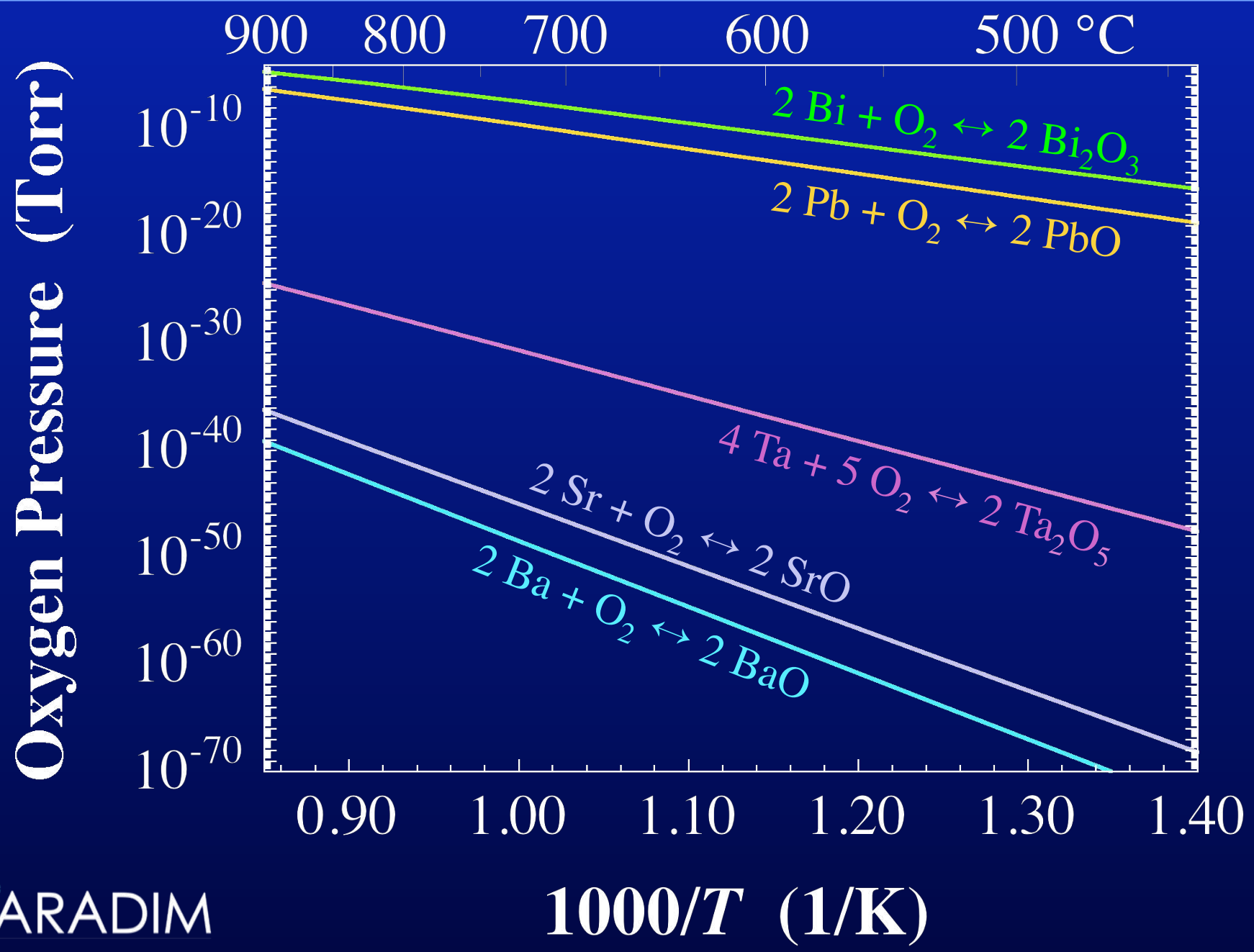

data from I. Barin, *Thermochemical Data of Pure Substances*, 3rd Ed., Vol. I and Vol. II (VCH, Weinheim, 1995).

PARADIM

NSF

O_2 Needed to Oxidize Constituents

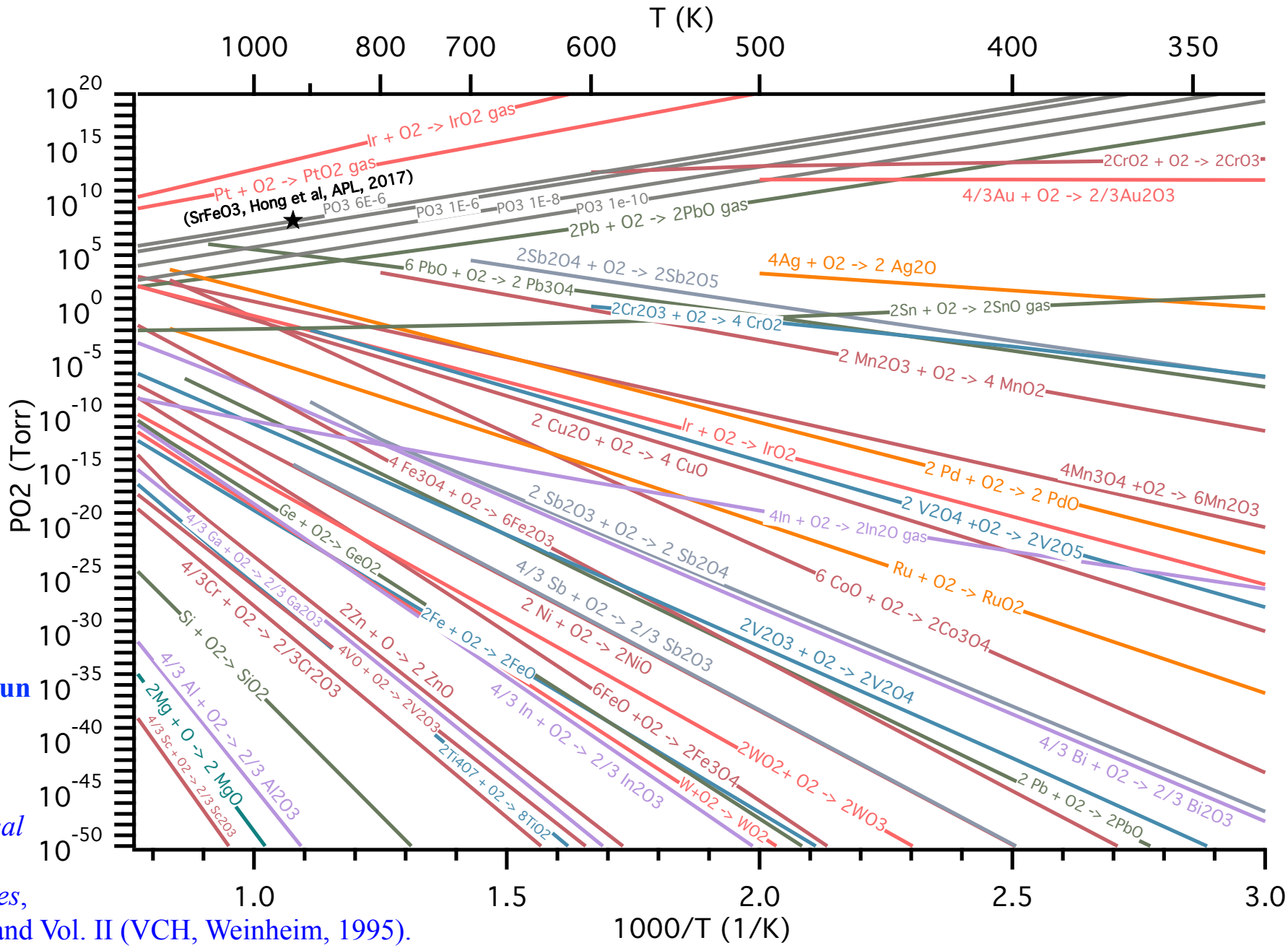

plot by **Jake Sun**

data from
I. Barin,
Thermochemical Data of Pure Substances,
3rd Ed., Vol. I and Vol. II (VCH, Weinheim, 1995).

$SrFeO_{3-x}$ Example with Ozone

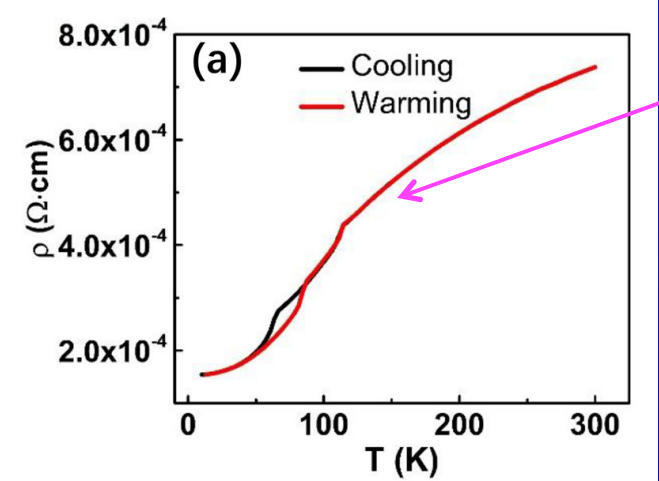

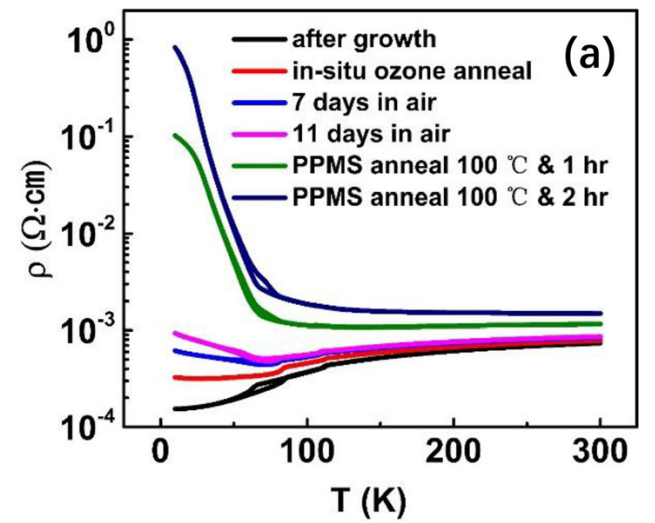

D. Hong, C. Liu, J. Pearson, and A. Bhattacharya, *Applied Physics Letters* **111** (2017) 232408.

As-grown (by MBE) ~$SrFeO_3$ film. Grown and cooled in 6×10^{-6} Torr of distilled ozone

$SrFeO_{3.00}$ single crystal annealed 5000 atm O_2 at 400 °C

$SrFeO_{2.95}$ single crystal annealed 750 atm O_2 at 400 °C

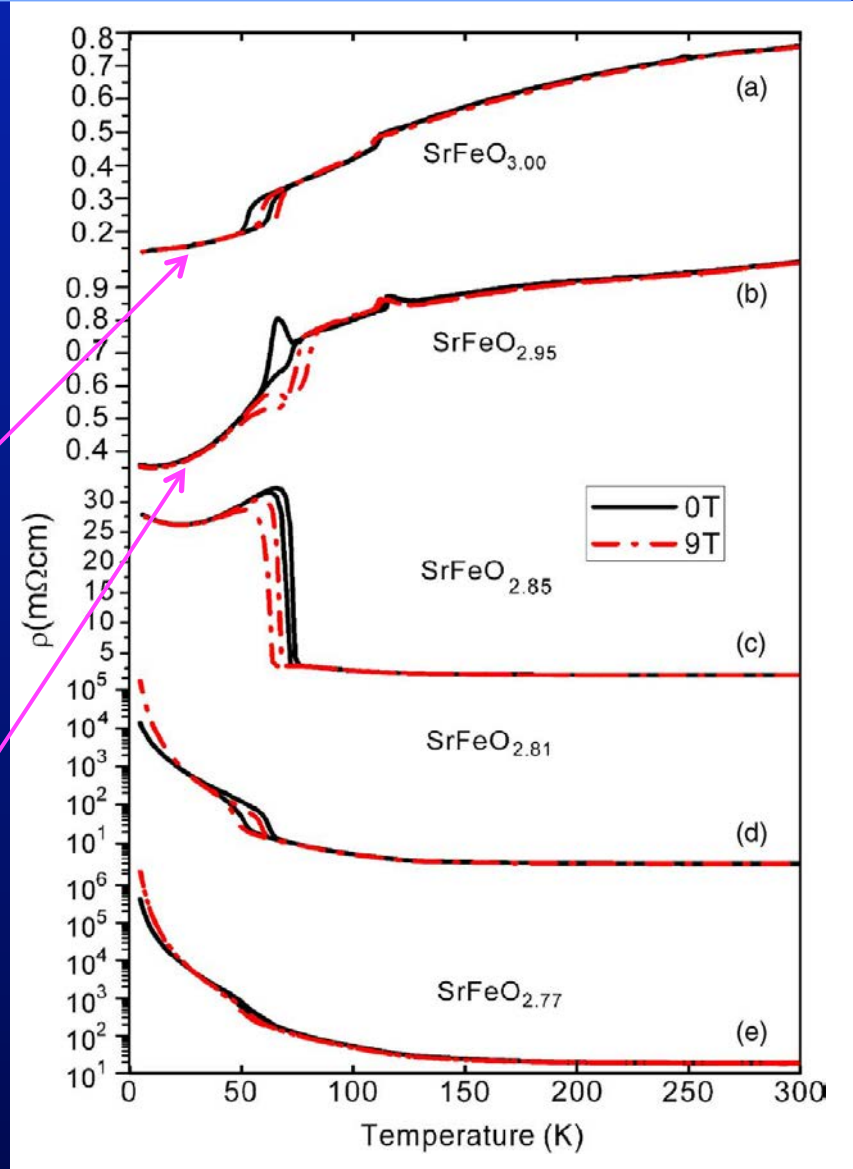

P. Adler, A. Lebon, V. Damljanović, C. Ulrich, C. Bernhard, A. Boris, A. Maljuk, C. Lin, and B. Keimer, *Physical Review B* **73** (2006) 094451.

PARADIM

NSF

O_2 Needed to Oxidize Cuprates

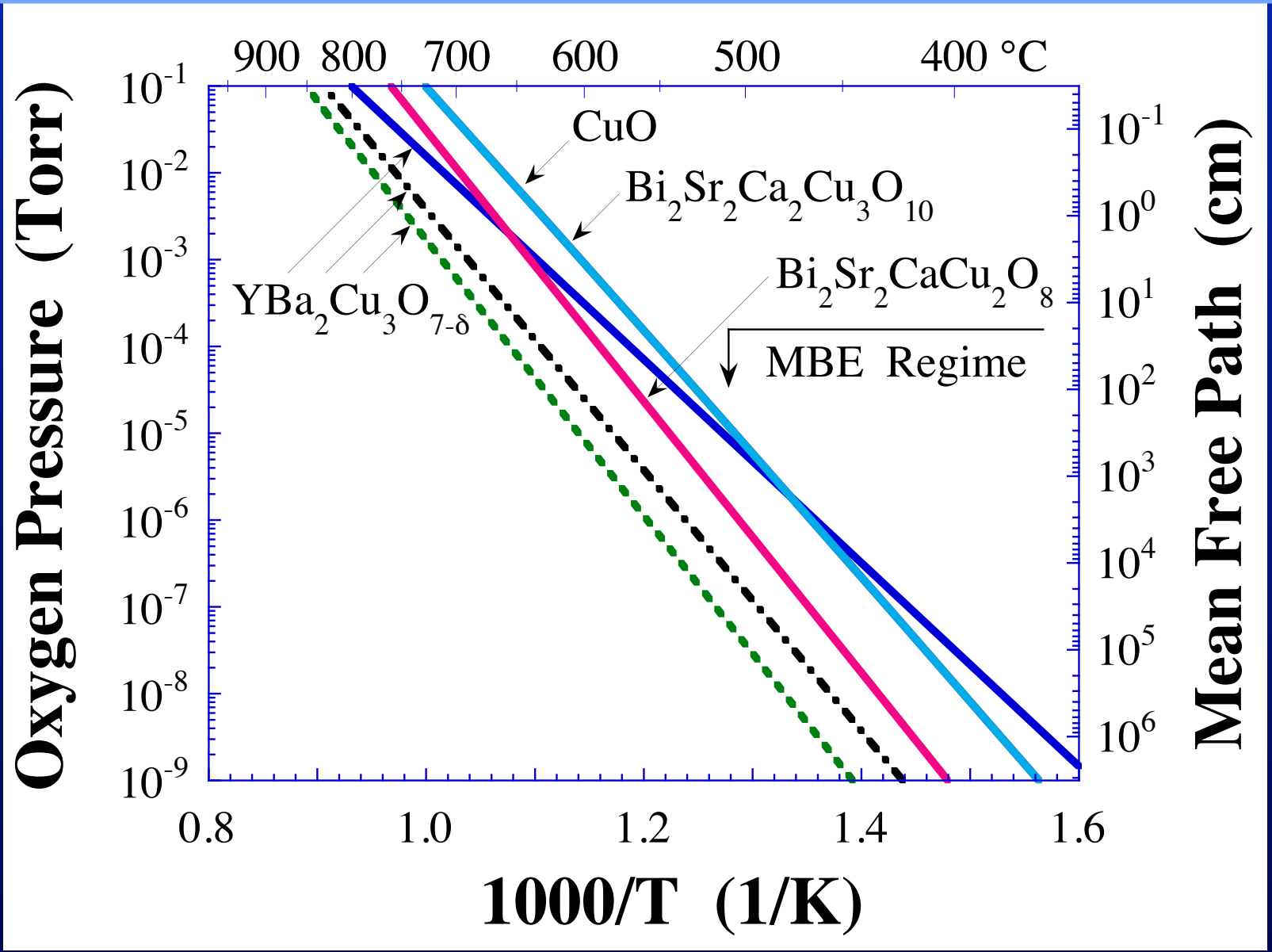

D.G. Schlom and J.S. Harris, Jr., in *Molecular Beam Epitaxy: Applications to Key Materials*, edited by R.F.C. Farrow (Noyes, Park Ridge, 1995), pp. 505-622.

Superior Oxidants to O_2

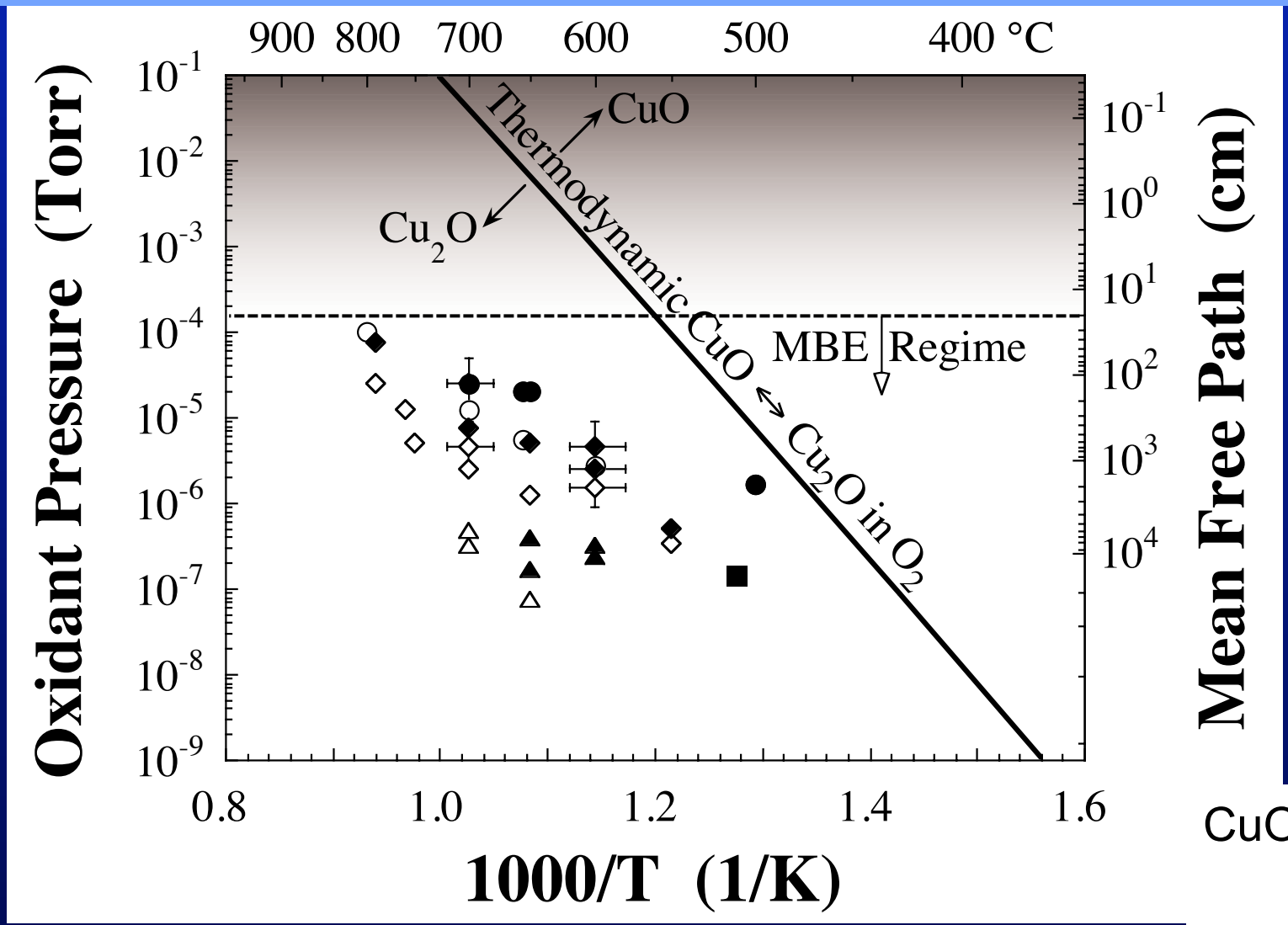

CuO formation in

- ▲ O
- ■ O^+
- ● NO_2
- ◆ O_3

D.G. Schlom and J.S. Harris, Jr., in *Molecular Beam Epitaxy: Applications to Key Materials*, edited by R.F.C. Farrow (Noyes, Park Ridge, 1995), pp. 505-622.

PARADIM

O_3 Activity by Thermodynamics

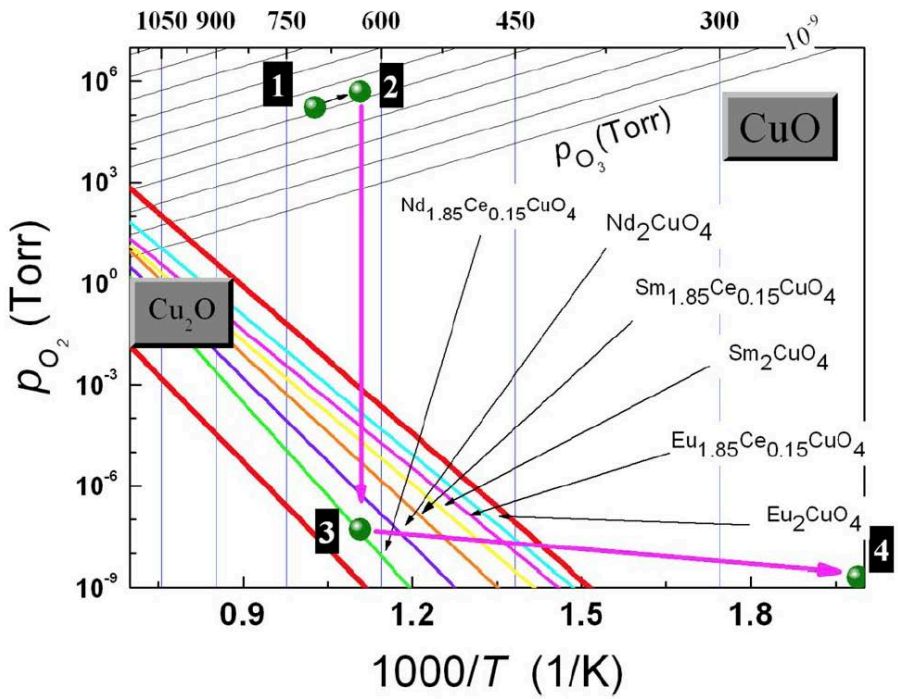

FIG. 1. (Color online) Typical thermodynamic phase stability diagram for electron-doped cuprates. Stability lines for CuO and Cu_2O have been calculated using the commercially available program MALT®. Additionally, the equilibria oxidizing potential lines for ozone and oxygen are calculated. The numbered points describe a typical growth of the thin film. The border lines for the different copper valencies are thick red colored. Between them, all experimentally established stability lines for the T'-structure compounds are lying. Points 1 and 2 represent the growth followed by annealing in vacuum (point 3) and afterwards cooled down to point 4.

$$O_2 \overset{\Delta G^\circ}{\longleftrightarrow} \frac{2}{3} O_3$$

$$P_{O_2} = P_{O_3}{}^{2/3} \; e^{\left(\frac{\Delta G^\circ}{R\,T_{sub}}\right)}$$

Activity of O_3 is ~10^{12} higher than O_2 at typical T_{sub}

Y. Krockenberger, J. Kurian, A. Winkler, A. Tsukada, M. Naito, and L. Alff, "Superconductivity Phase Diagrams for the Electron-Doped Cuprates $R_{2-x}Ce_xCuO_4$ (R=La , Pr, Nd, Sm, and Eu)," *Physical Review B* **77** (2008) 060505.

Oxygen vs. Ozone

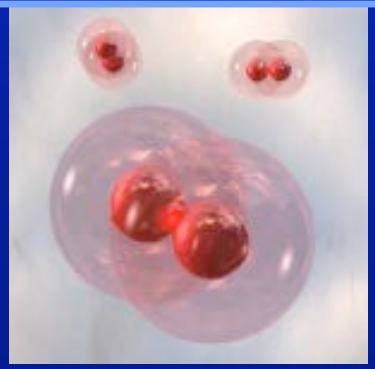

Oxygen:

- Easy to use – directly from the cylinder
- Depending on material, films are oxygen-deficient

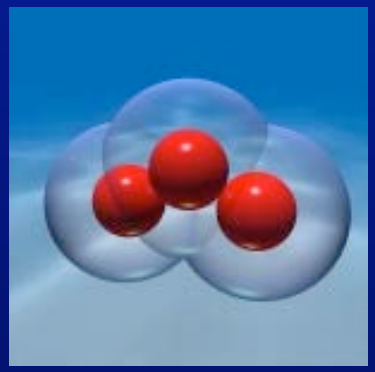

Ozone from ozone generator:

- Around 15 wt% O_3 in O_2
- As O_3 easily decomposes, one O_3 is similar to one O radical
- Higher wt% not achievable, saturation of O_3 concentration

Distilled ozone:

- Can provide 80-100 wt% pure O_3
- Better film oxidation, wider process window
- But: Gas is explosive above ~10 Torr (absolute), liquid is explosive and shock-sensitive

PARADIM

NSF

Vapor Pressure Oxygen vs. Ozone

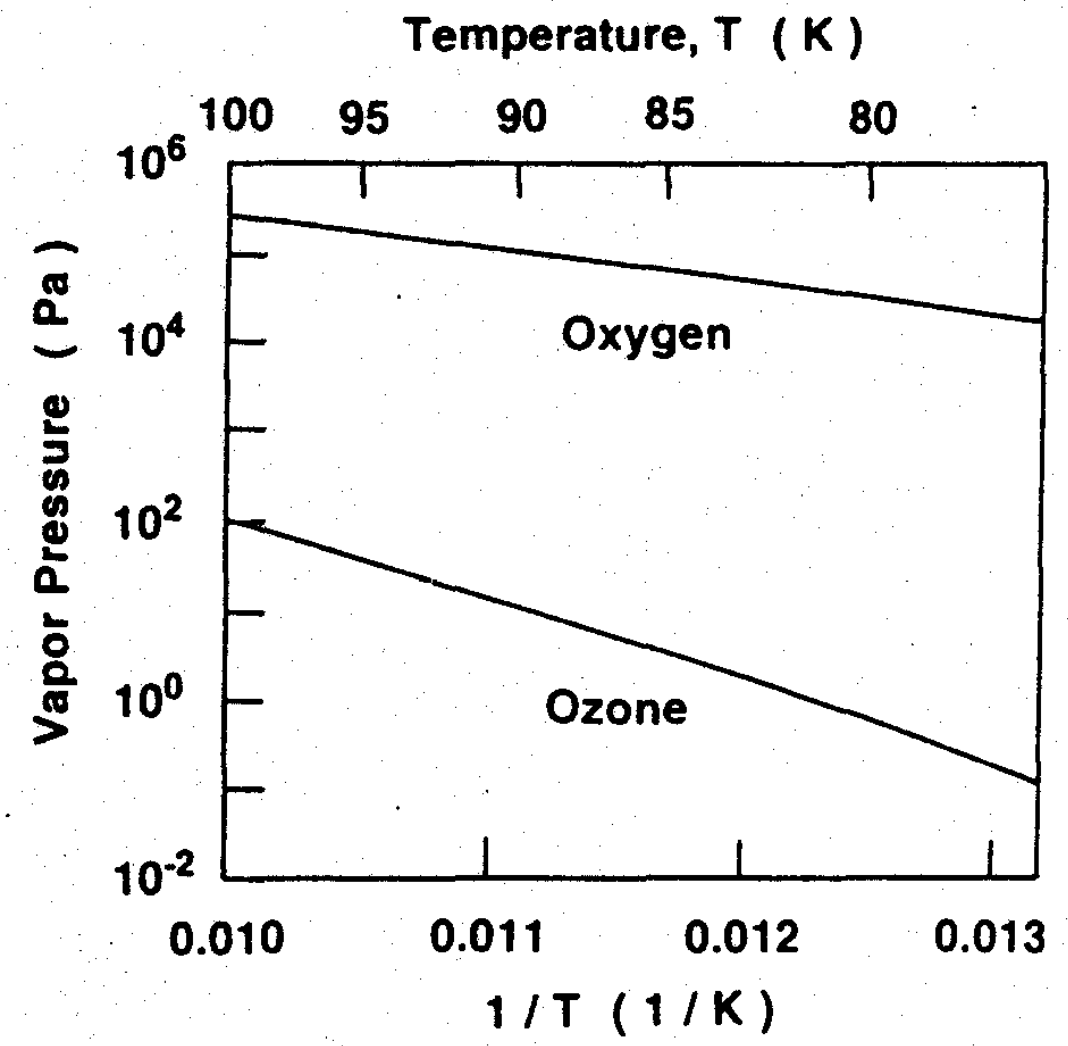

FIG. 4. Vapor pressure of ozone and oxygen as a function of temperature.

S. Hosokawa, and S. Ichimura, "Ozone Jet Generator as an Oxidizing Reagent Source for Preparation of Superconducting Oxide Thin Film," *Review of Scientific Instruments* **62** (1991) 1614-1619.

Ozone Safety Concerns

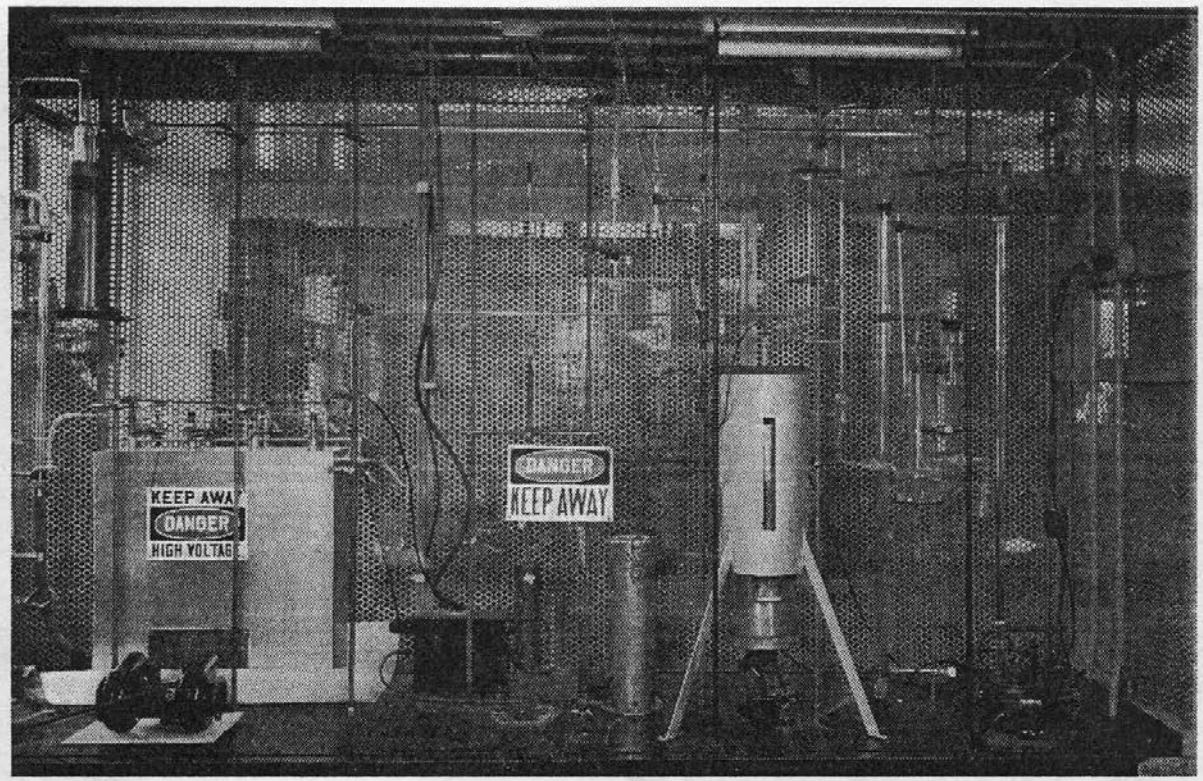

Figure 4. Ozone system

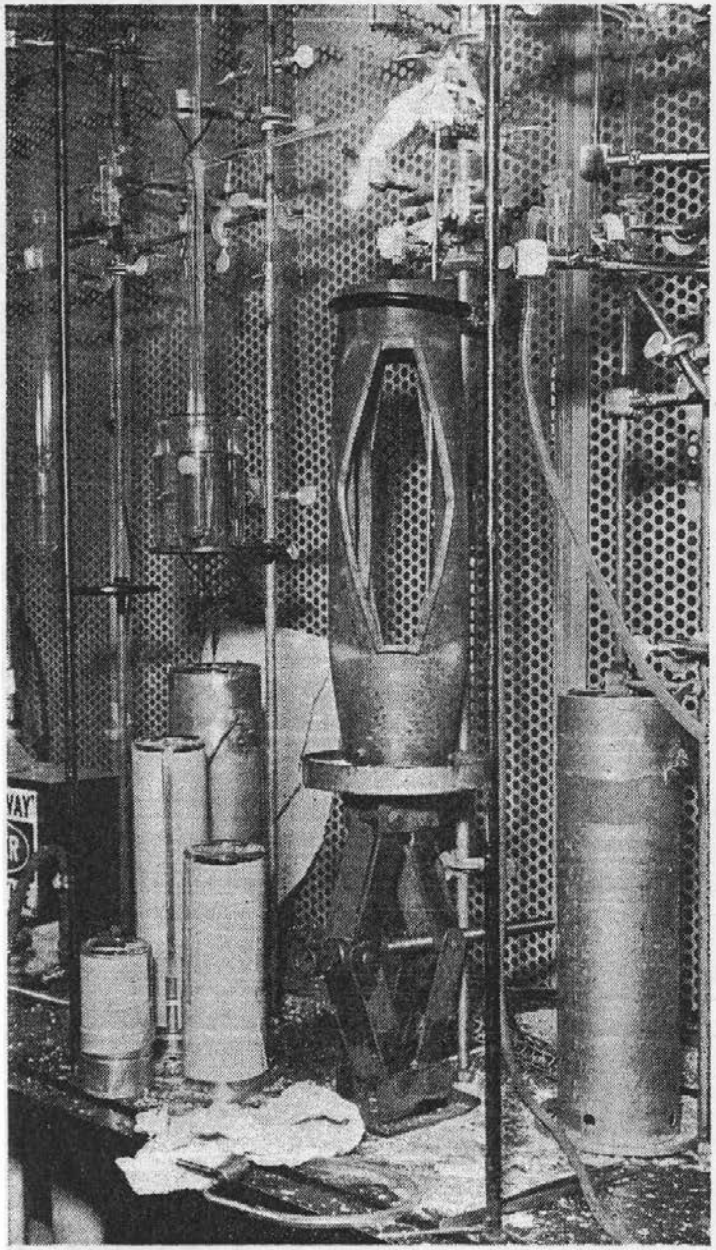

Figure 5. Apparatus after explosion

A.C. Jenkins
"Laboratory Techniques for Handling High-Concentration Liquid Ozone," in:
Ozone Chemistry and Technology
Vol. 21 of Advances in Chemistry Series
(American Chemical Society, Washington, D.C., 1959) pp. 13-21.

PARADIM

Ozone Safety Concerns

OZONE FOR ROCKETS

Concentrated liquid ozone has been proposed as a rocket fuel by Prof. Clark E. Thorp of the Illinois Institute of Technology, who recently disclosed advances made at the Institute by which ozone can be handled with safety. Ozone is a form of oxygen with three atoms to the molecule instead of two as in ordinary life-supporting oxygen. By demonstrating that it can be safely manufactured, Professor Thorp stated, the door has been opened for tonnage production. During World War II, German scientists worked overtime on an ozone-propelled rocket designed to bombard New York City from European launching platforms. But they were unable to discover the secret of handling ozone without spontaneous detonation.

"Ozone for Rockets,"
Ordnance: The Journal of the Army Ordnance Association **36** [187]
(July-August 1951) pp. 108-110.

Ozone Distillation (U. Minnesota)

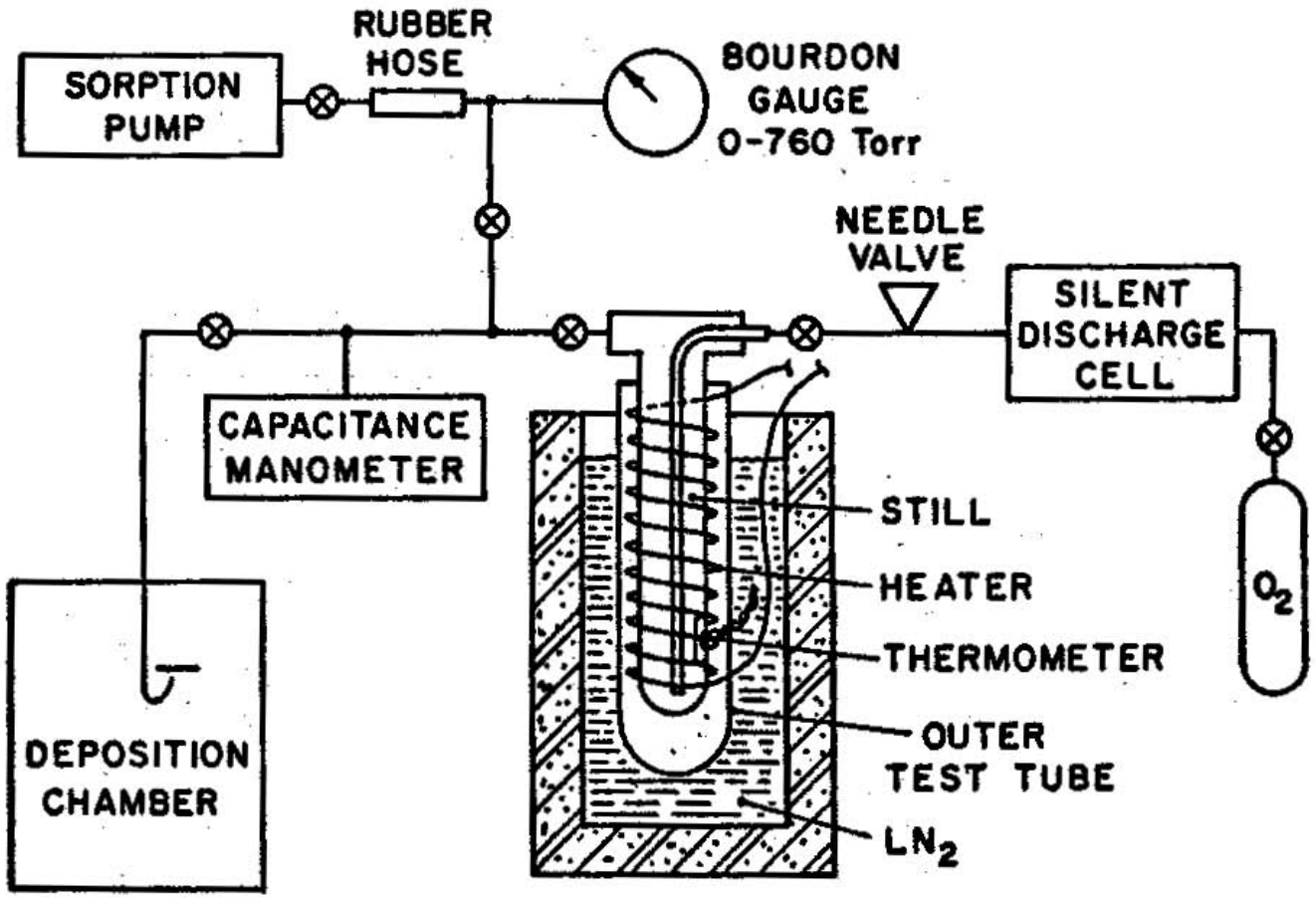

FIG. 1. Ozone-production and storage apparatus. During production of ozone, the still heater is off and the outer test tube surrounding the still is filled with liquid nitrogen.

D.D. Berkley, A.M. Goldman, B.R. Johnson, J. Morton, and T. Wang, "Techniques for the Growth of Superconducting Oxide Thin Films Using Pure Ozone Vapor," *Review of Scientific Instruments* **60** (1989) 3769-3774.

Ozone in Silica Gel (Union Carbide)

Separation of Ozone from Oxygen by a Sorption Process

G. A. COOK, A. D. KIFFER, C. V. KLUMPP, A. H. MALIK, and L. A. SPENCE

Research and Development Laboratory, Linde Co., A Division of Union Carbide Corp., Tonawanda, N. Y.

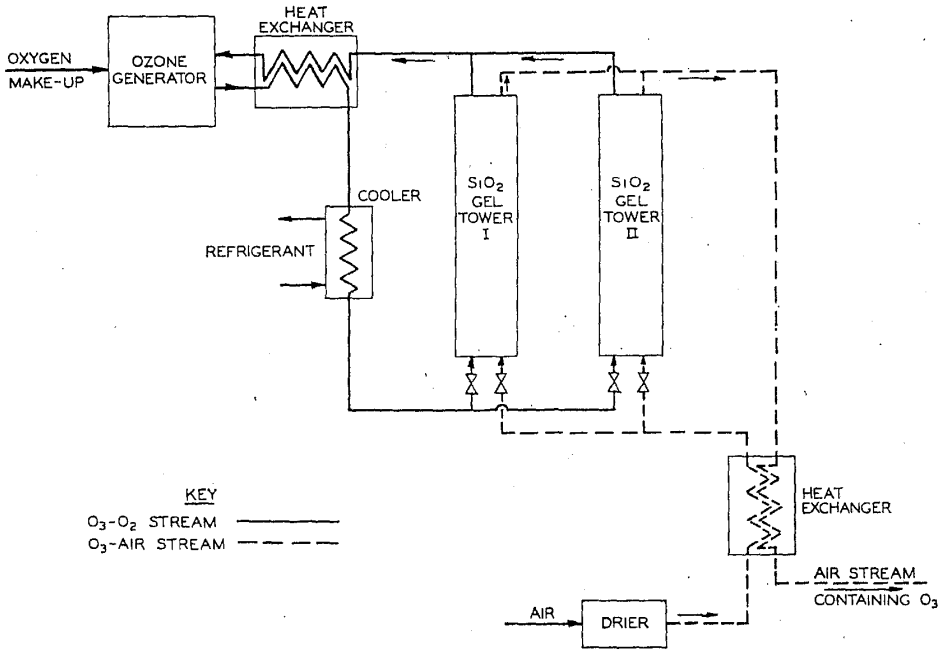

Figure 7. Simplified flow diagram for two-stage transfer process

Ozone is separated from oxygen by adsorption on refrigerated silica gel, followed by desorption, either in pure form at reduced pressure, or diluted by air, nitrogen, argon, or other gas not strongly adsorbed on silica gel. This is a practical method, free from hazard when correctly performed.

G.A. Cook, A.D. Kiffer, , C.V. Klumpp, A.H. Malik, and L.A. Spence, "Separation of Ozone from Oxygen by a Sorption Process," in: *Ozone Chemistry and Technology*, Vol. 21 of Advances in Chemistry Series, (American Chemical Society, Washington, D.C., 1959) pp. 44-52.

PARADIM

Ozone in Silica Gel (Union Carbide)

Safety Tests

An electric spark was passed between two tungsten electrodes within the gel bed. No explosions took place at −105° C. with loadings as high as 21 grams of ozone per 100 grams of gel.

A piece of fine iron wire was placed in the bed of gel and ignited by passing an electric current through it. With a loading of 9 grams of ozone per 100 grams of gel, a test was made at −78° C. After ignition of the wire, a glow in the vessel was observed, but no explosion took place. With a loading of 20 grams of ozone per 100 grams of gel at −105° C., a dull pop was heard when the wire was ignited, most of the ozone changed to oxygen, and the gel was extensively pulverized. The glass container was broken but not shattered.

G.A. Cook, A.D. Kiffer, , C.V. Klumpp, A.H. Malik, and L.A. Spence, "Separation of Ozone from Oxygen by a Sorption Process," in: *Ozone Chemistry and Technology*, Vol. 21 of Advances in Chemistry Series, (American Chemical Society, Washington, D.C., 1959) pp. 44-52.

PARADIM

NSF

Ozone in Silica Gel

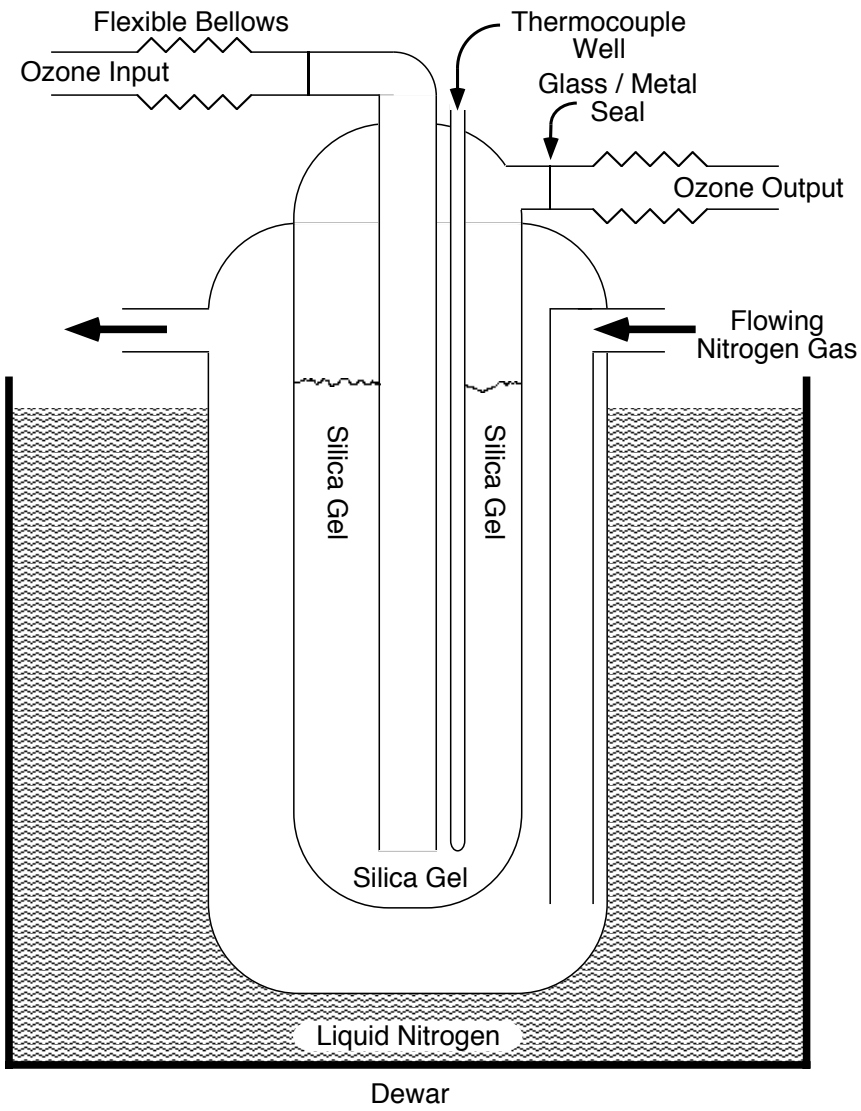

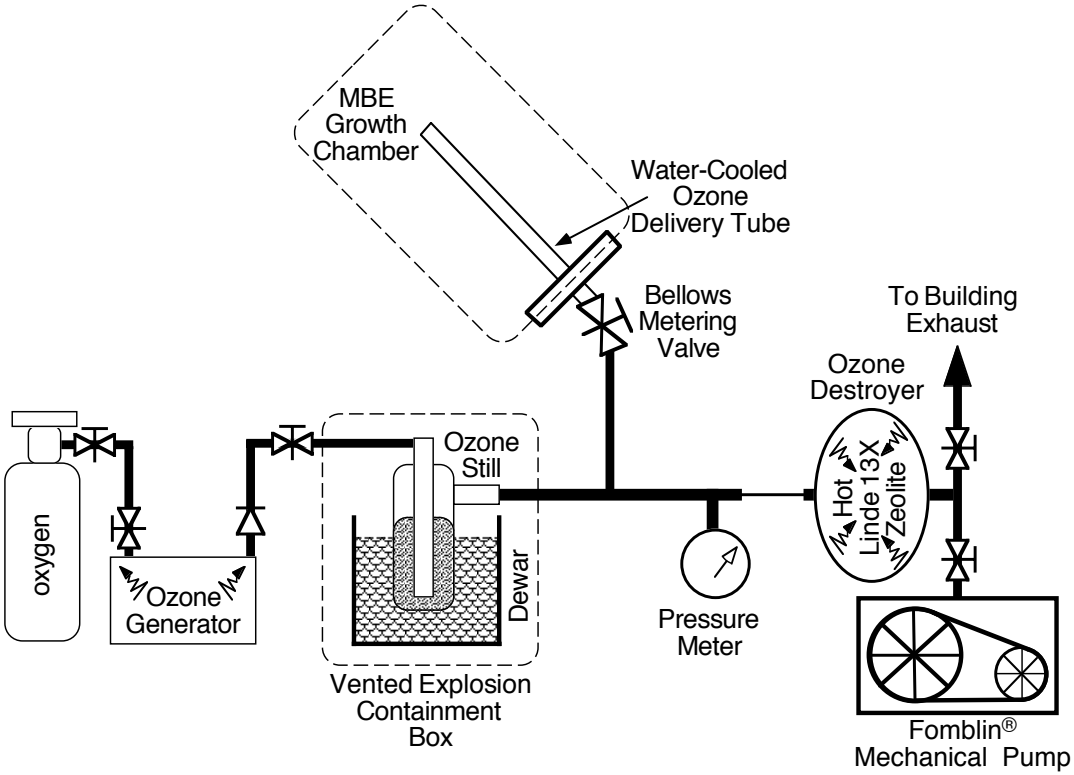

D.G. Schlom and J.S. Harris, Jr., in *Molecular Beam Epitaxy: Applications to Key Materials*, edited by R.F.C. Farrow (Noyes, Park Ridge, 1995), pp. 505-622.

Process Control

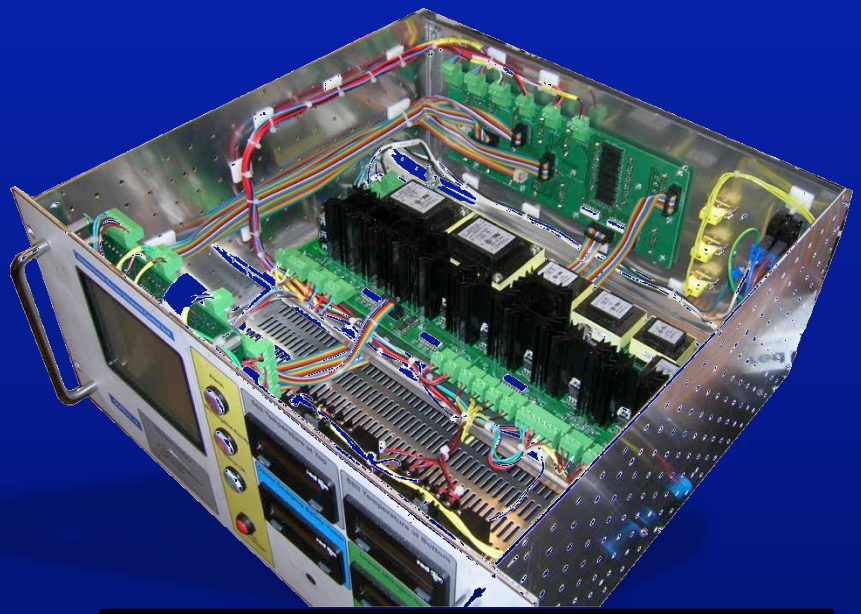

- Safety committee requirements led to development of fully integrated process controller
- Controller monitors all process equipment and parameters
- Countermeasures if close to critical limit
- Self-test of equipment before process start
- Fully automated operation
- No need to manually watch ozone process, user can focus on MBE growth!!!

Ozone System Passivation

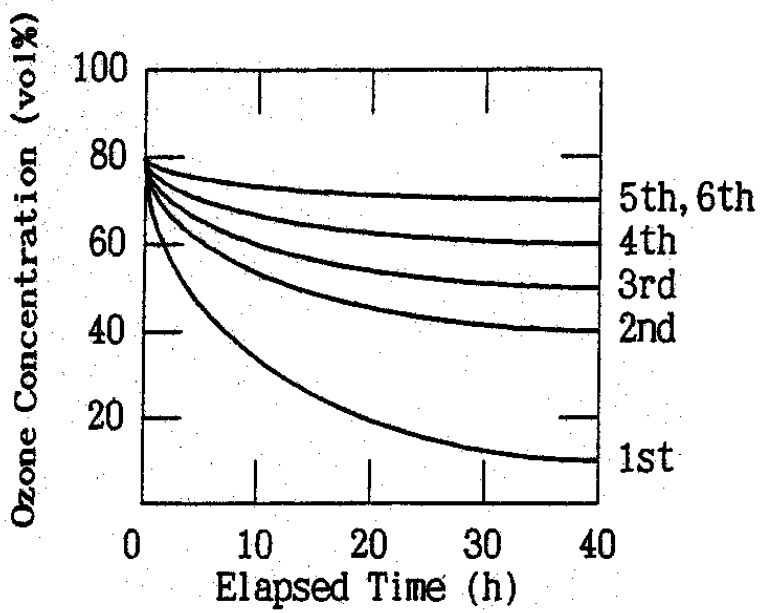

Fig. 2. Ozone concentration decay during ozone passivation.

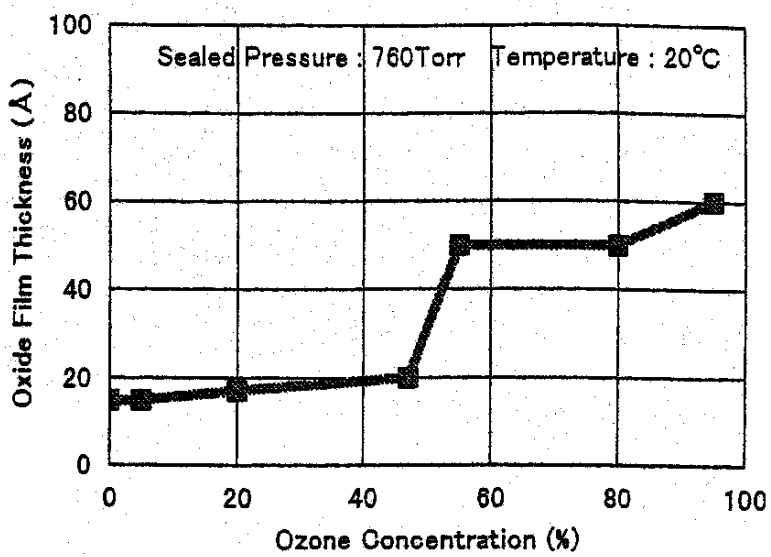

Fig. 4. Relationship of ozone concentration with thickness of passivated film formed at atmospheric pressure and 20°C.

K. Koike, G. Inoue, T. Takata, and T. Fukuda,
Ozone Passivation Technique for Corrosive Gas Distribution System,"
Japanese Journal of Applied Physics **36** (1997) 7437-7441.

Pros and Cons of Ozone

- Pros
  - Excellent Oxidant ($>10^3$ (experiment) to $<10^{12}$ (thermo) more powerful than O_2)
  - 80% Ozone (+20% O_2) delivered to the Substrate
  - No Energetic Species (thermal ozone beam)
  - Clean (lower in contaminants than plasma beam)
- Cons
  - Safety (Ozone still issues)
  - Safety (Pump issues)
  - Need Ozone-Compatible UHV Leak Valve
  - Need to Passivate Ozone System

PARADIM

NSF

If you want to grow EuO by MBE, what oxidant should you use?

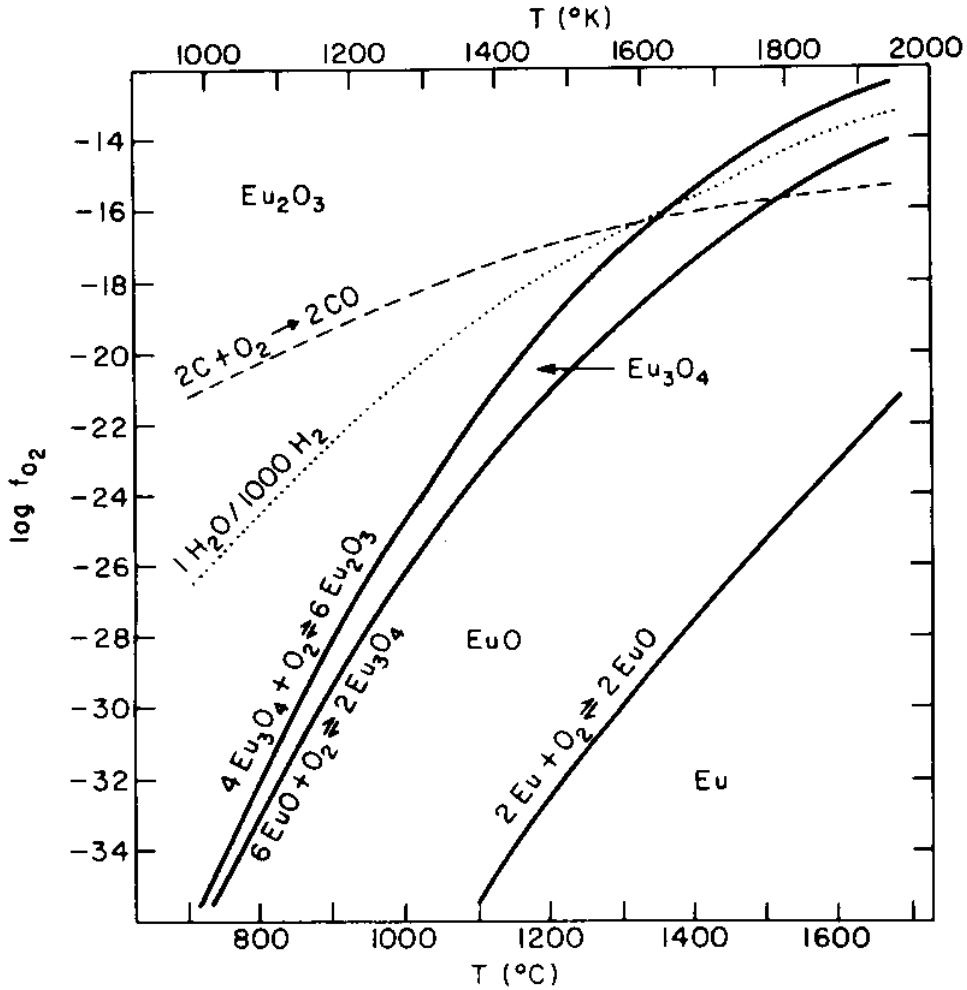

Fig. 1. Plot of $f_{O_2}(T)$ for oxidation reactions of Eu, EuO, and Eu_3O_4 and for C to CO and H_2 with 1 part/1000 H_2O.

G.J. McCarthy
"Oxygen-Fugacity–Temperature Diagram for the Eu-O System," *Journal of the American Ceramic Society* **57** (1974) 502.

PARADIM

NSF

Nuts and Bolts of Oxide MBE

- Mean Free Path (maximum P_{O_2})
- Minimum P_{O_2}, need for P_{O_3}
- Optimal T_{sub}
- MBE System
- MBE Sources
- Crucibles

PARADIM

NSF

Surface vs. Bulk Diffusion

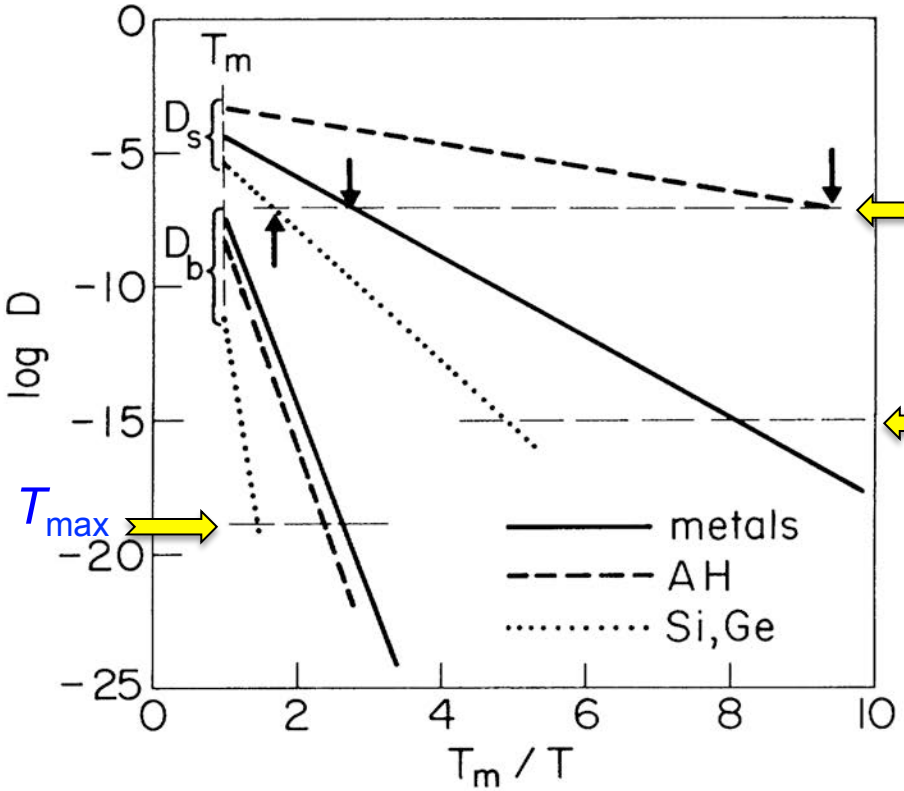

Assuming growth rate of 0.1 monolayer/sec

T_{min} for smooth epitaxial films (growth by step propagation)

T_{min} for epitaxy

FIG. 6. Diagram showing deduced global dependences of surface and bulk diffusion coefficients, D_s and D_b, on T_m/T for metals (solid lines), elemental semiconductors (dotted lines), and salts (dashed lines). The construction is described in the text. Smooth flat interfaces generally require $D_s \gtrsim 10^{-8}$–10^{-7} cm^2/sec, which fixes the lowest growth temperatures (arrows) as $\sim 3T_m/8$, $0.55T_m$, and $0.1T_m$ in the three cases. RHEED oscillations are expected for $D_s \gtrsim 10^{-15}$ cm^2/sec and bulk interdiffusion for $D_b \gtrsim 10^{-19}$ cm^2/sec.

Optimal Growth Temperatures

$$0.55 < \frac{T_{sub}}{T_{melt}} < 0.7 \text{ for semiconductors}$$

$$0.35 < \frac{T_{sub}}{T_{melt}} < 0.4 \text{ for metals}$$

$$0.1 < \frac{T_{sub}}{T_{melt}} < 0.4 \text{ for simple ceramics}$$

M.H. Yang and C.P. Flynn
Physical Review Letters **62** (1989) 2476-2479.

Universal Diffusion Behavior of Metals

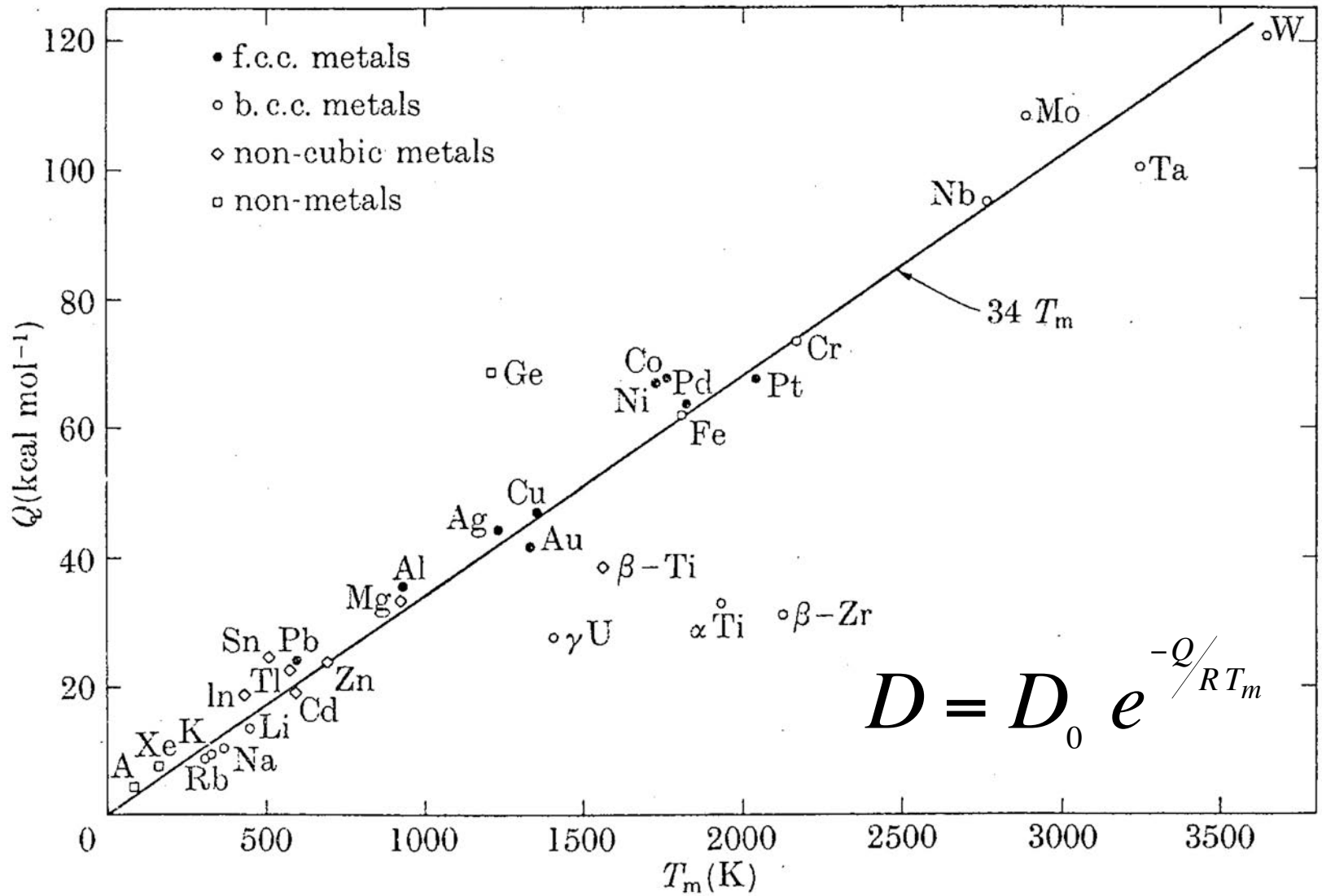

$$D = D_0 \, e^{-Q/RT_m}$$

FIG. 14.31. The correlation between Q and T_m.

C. Peter Flynn, *Point Defects and Diffusion* (Oxford, 1972) pp. 783-785.

Determining Surface Diffusion from RHEED Oscillations

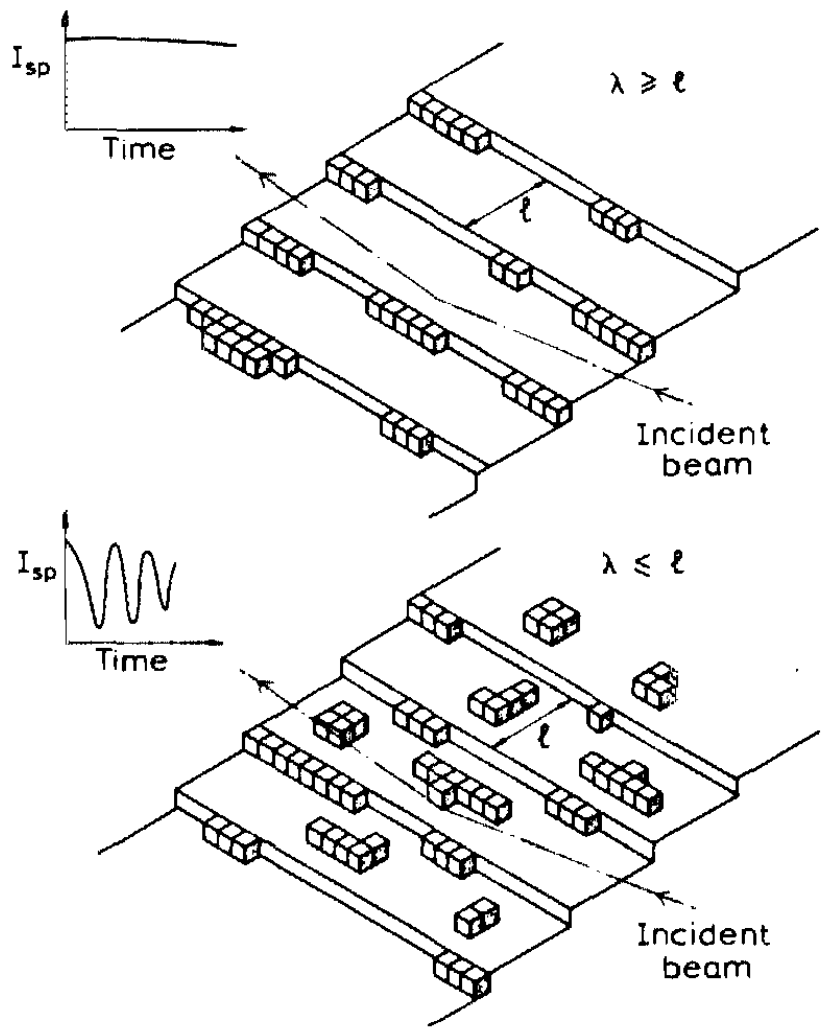

FIG. 1. Schematic illustration of the principle of the method, showing the change in RHEED information as the growth mode changes from "step flow" to 2-D nucleation. Steps lie along [100].

J.H. Neave, P.J. Dobson, B.A. Joyce, and J. Zhang, *Applied Physics Letters* **47** (1985) 100-102.

Surface vs. Bulk Diffusion

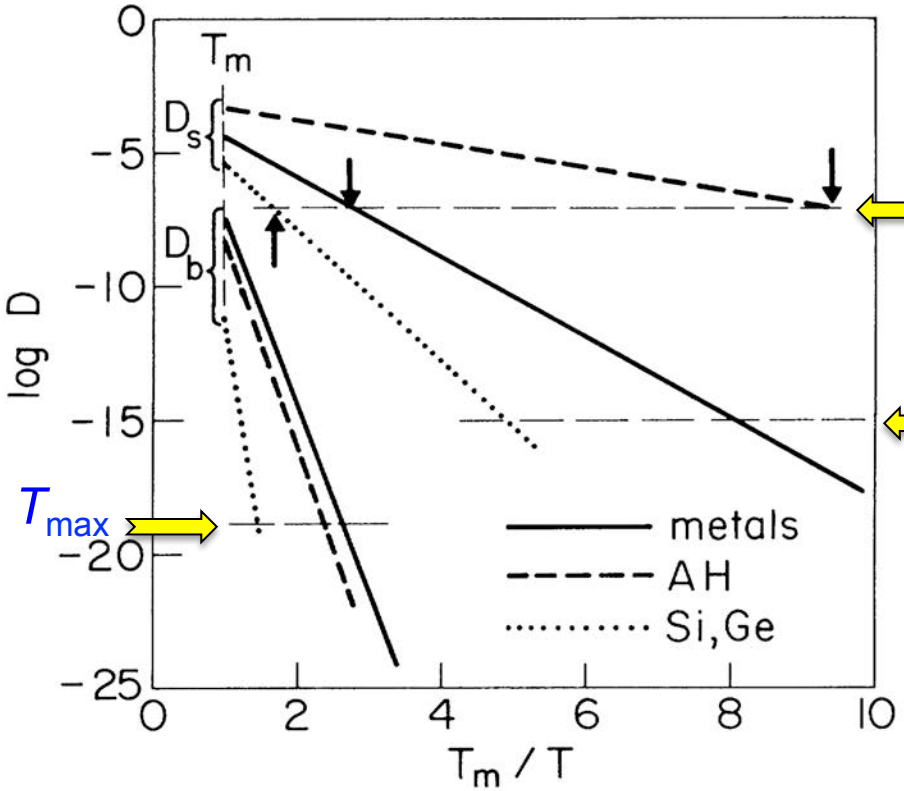

Assuming growth rate of 0.1 monolayer/sec

T_{min} for smooth epitaxial films (growth by step propagation)

T_{min} for epitaxy

FIG. 6. Diagram showing deduced global dependences of surface and bulk diffusion coefficients, D_s and D_b, on T_m/T for metals (solid lines), elemental semiconductors (dotted lines), and salts (dashed lines). The construction is described in the text. Smooth flat interfaces generally require $D_s \gtrsim 10^{-8}$–10^{-7} cm^2/sec, which fixes the lowest growth temperatures (arrows) as $\sim 3T_m/8$, $0.55T_m$, and $0.1T_m$ in the three cases. RHEED oscillations are expected for $D_s \gtrsim 10^{-15}$ cm^2/sec and bulk interdiffusion for $D_b \gtrsim 10^{-19}$ cm^2/sec.

Optimal Growth Temperatures

$$0.55 < \frac{T_{sub}}{T_{melt}} < 0.7 \text{ for semiconductors}$$

$$0.35 < \frac{T_{sub}}{T_{melt}} < 0.4 \text{ for metals}$$

$$0.1 < \frac{T_{sub}}{T_{melt}} < 0.4 \text{ for simple ceramics}$$

M.H. Yang and C.P. Flynn
Physical Review Letters **62** (1989) 2476-2479.

Surface Energy Considerations

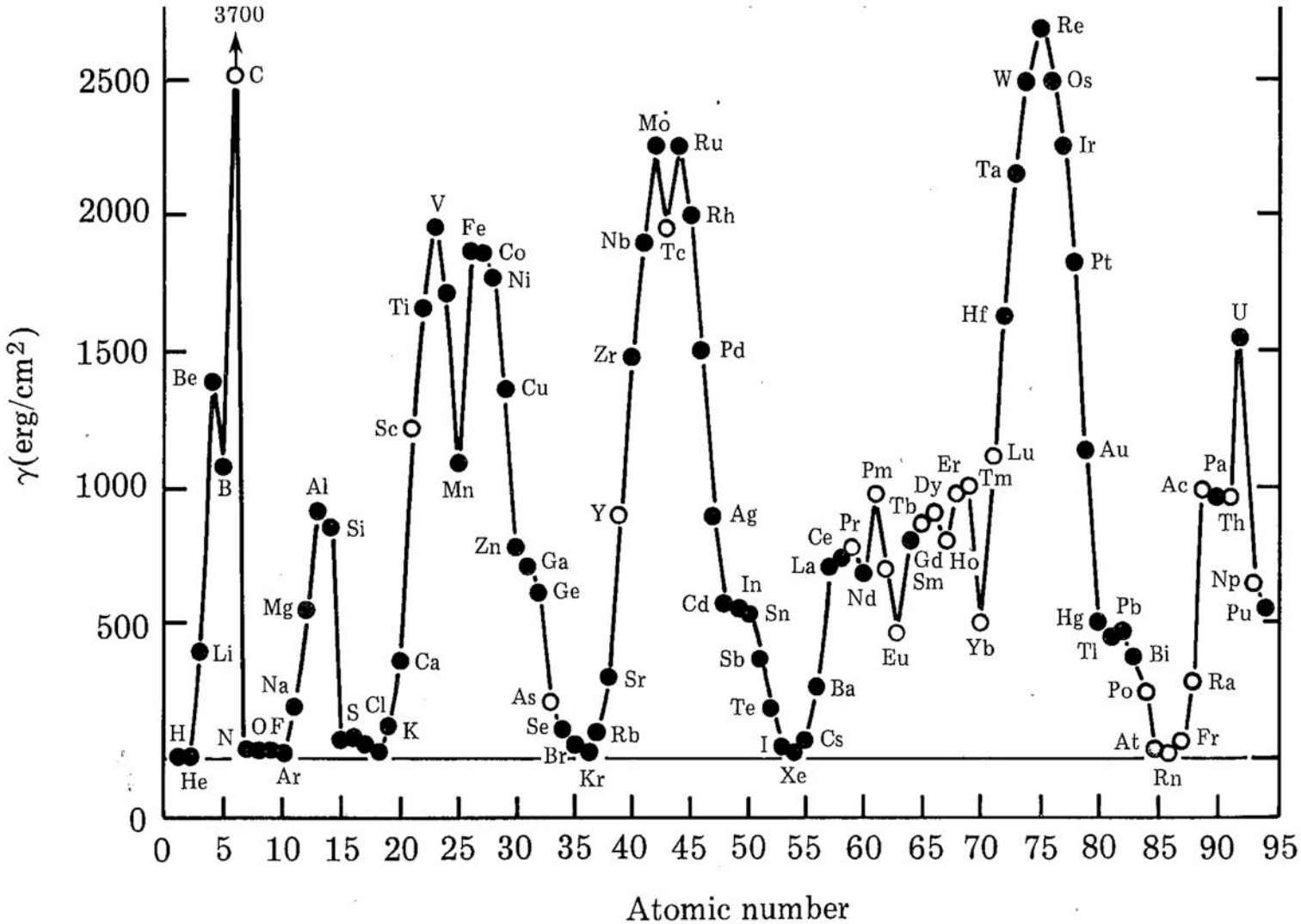

FIGURE 2.7 Surface tension of elements in the liquid phase (from Zangwill, 1988).

K.-N. Tu, J.W. Mayer, and L.C. Feldman,
Electronic Thin Film Science for Electrical Engineers and Materials Scientists
(Macmillan, 1992).

TEM of MBE-Grown Superlattices

AlAs / GaAs

A.K. Gutakovskii *et al.*,
Phys. Stat. Sol. (a) **150** (1995) 127.

$PbTiO_3$ / $SrTiO_3$

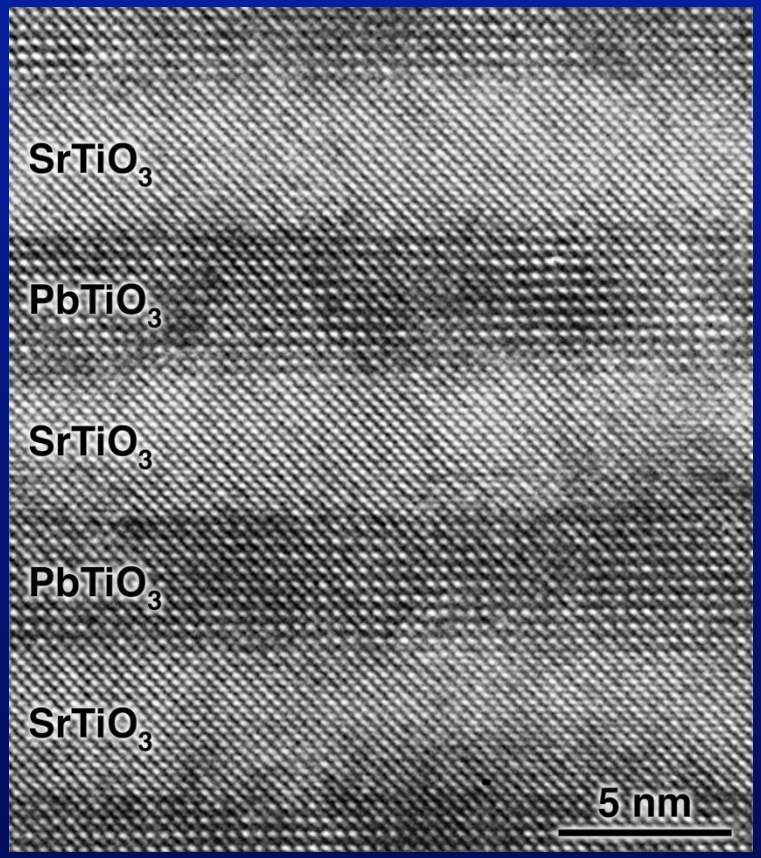

C.D. Theis
(1st Generation Schlom Group)

$BaTiO_3$ / $SrTiO_3$

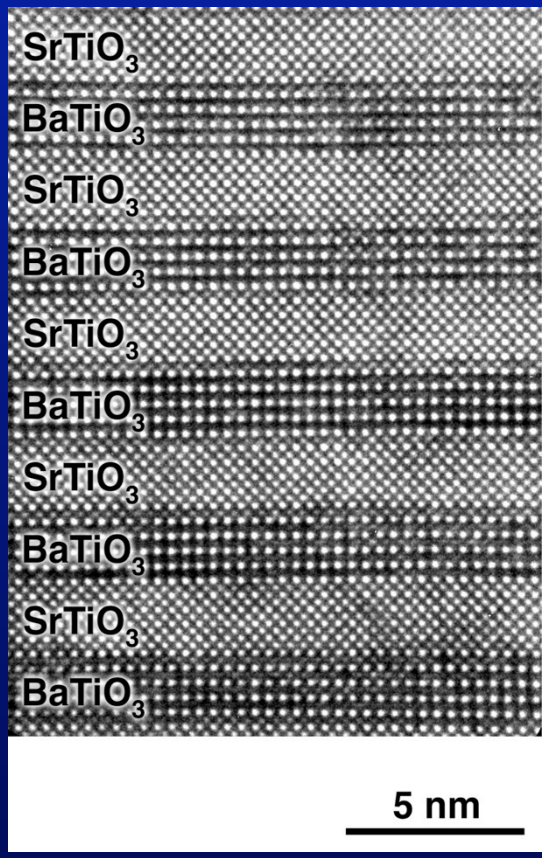

J.H. Haeni
(2nd Generation)

HRTEM—Pan Group (Michigan)
D.G. Schlom *et al.*, Mater. Sci. Eng. B **87** (2001) 282.

PARADIM

NSF

From the observed morphology, which likely has the <u>higher</u> surface energy?

(a) GaAs

(b) AlAs

(c) They appear to have the same surface energies

PARADIM

NSF

Thermodynamic Considerations

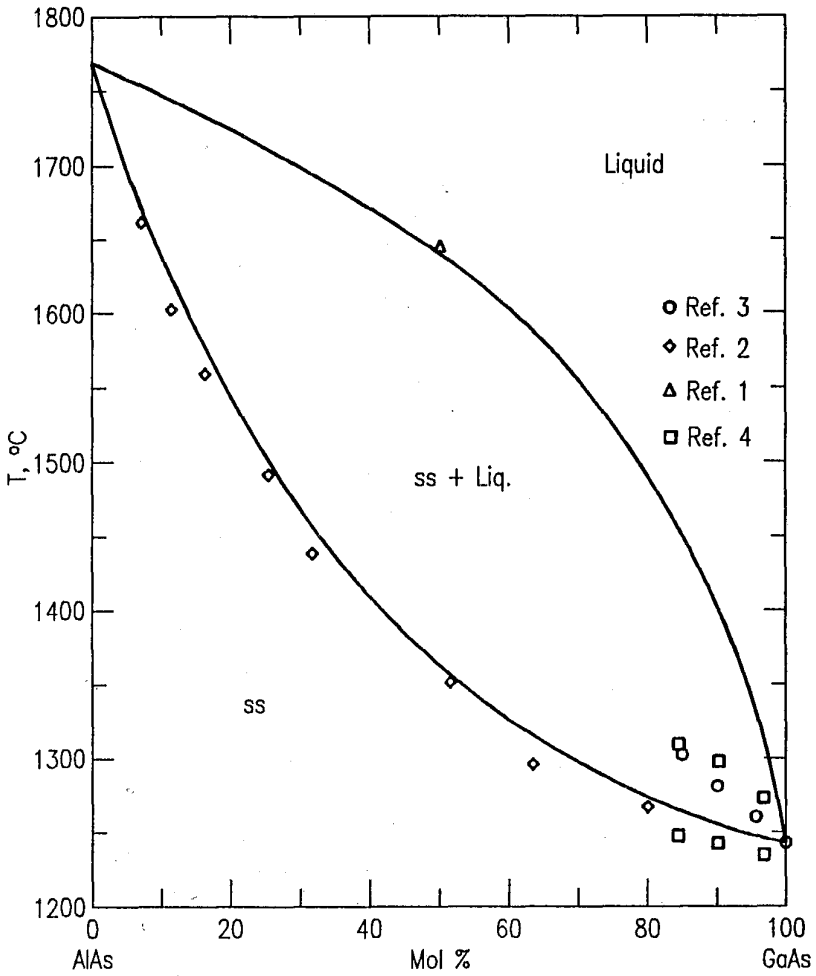

Fig. 8343—Pseudobinary system AlAs-GaAs.
K. Y. Ma, S. H. Li, and G. B. Stringfellow, "P, As, and Sb Phase Diagrams", Special Report to the Standard Reference Data Program, National Institute of Standards and Technology; Gaithersburg, Maryland (1987).

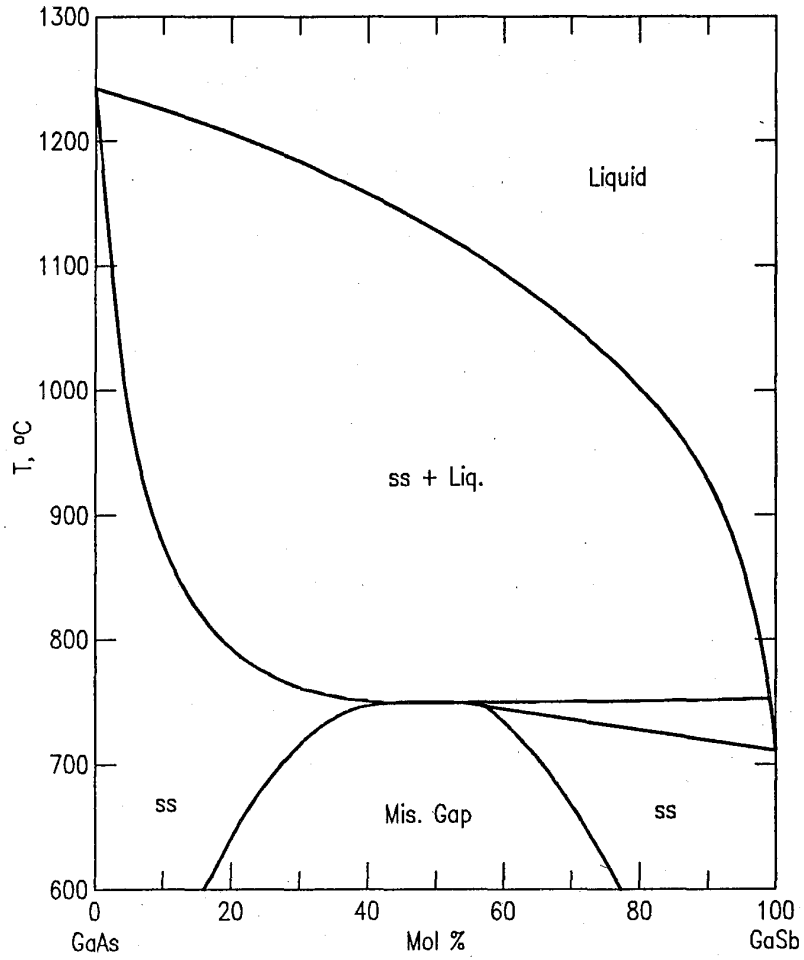

Fig. 8362—Pseudobinary system GaAs-GaSb. Calculated diagram.
K. Y. Ma, S. H. Li, and G. B. Stringfellow, "P, As, and Sb Phase Diagrams", Special Report to the Standard Reference Data Program, National Institute of Standards and Technology; Gaithersburg, Maryland (1987).

PARADIM

Phase Diagrams for Ceramists, Vol. 9, edited by G.B. Stringfellow (American Ceramic Society, Westerville, 1992).

NSF

Thermodynamic Considerations

Increased Interface Roughness and Clustering at Non-Optimal Growth Conditions

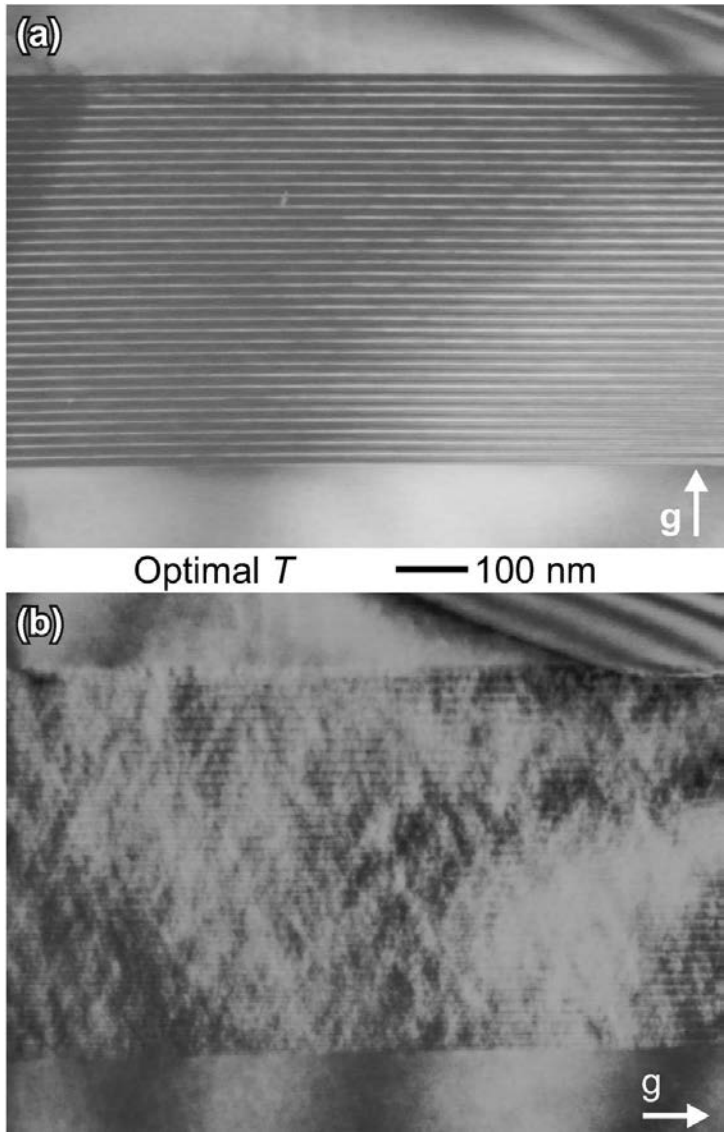

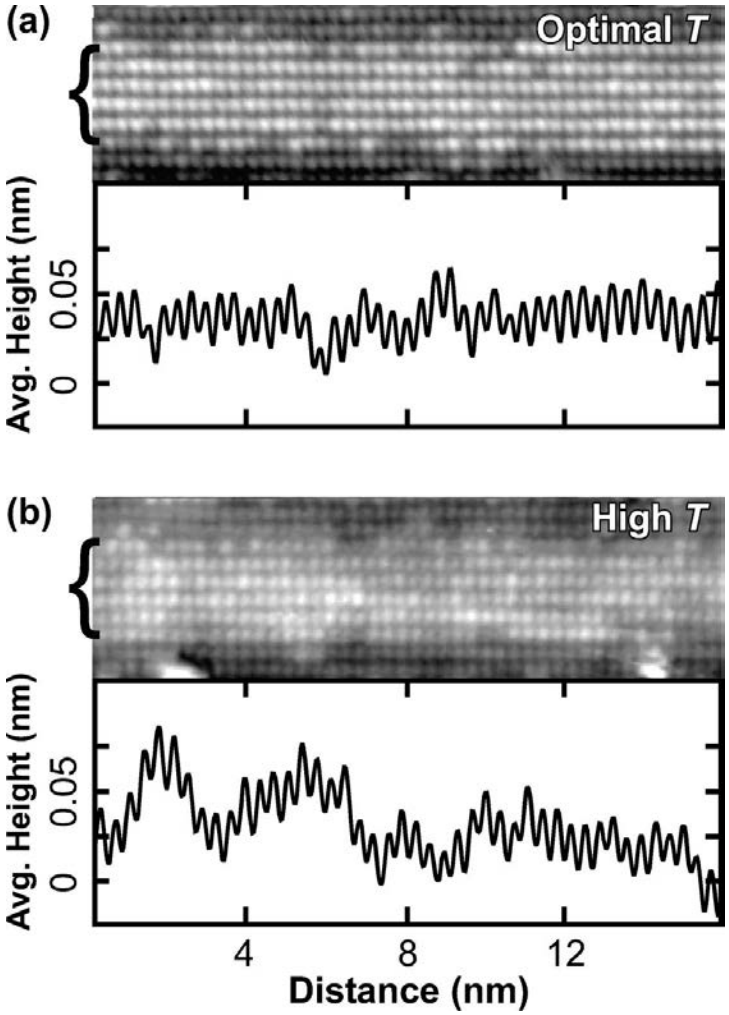

FIG. 6. XSTM images and average-height profiles for InGaSb-alloy layers in an (a) optimal- and (b) high-temperature sample. (a) −2.0 V, 50 pA and (b) −2.5 V, 0.5 nA.

W. Barvosa-Carter, M.E. Twigg, M.J. Yang, and L.J. Whitman
Physical Review B **63** (2001) 245311.

Nuts and Bolts of Oxide MBE

- Mean Free Path (maximum P_{O_2})
- Minimum P_{O_2}, need for P_{O_3}
- Optimal T_{sub}
- MBE System
- MBE Sources
- Crucibles

PARADIM

NSF

Oxide MBE System

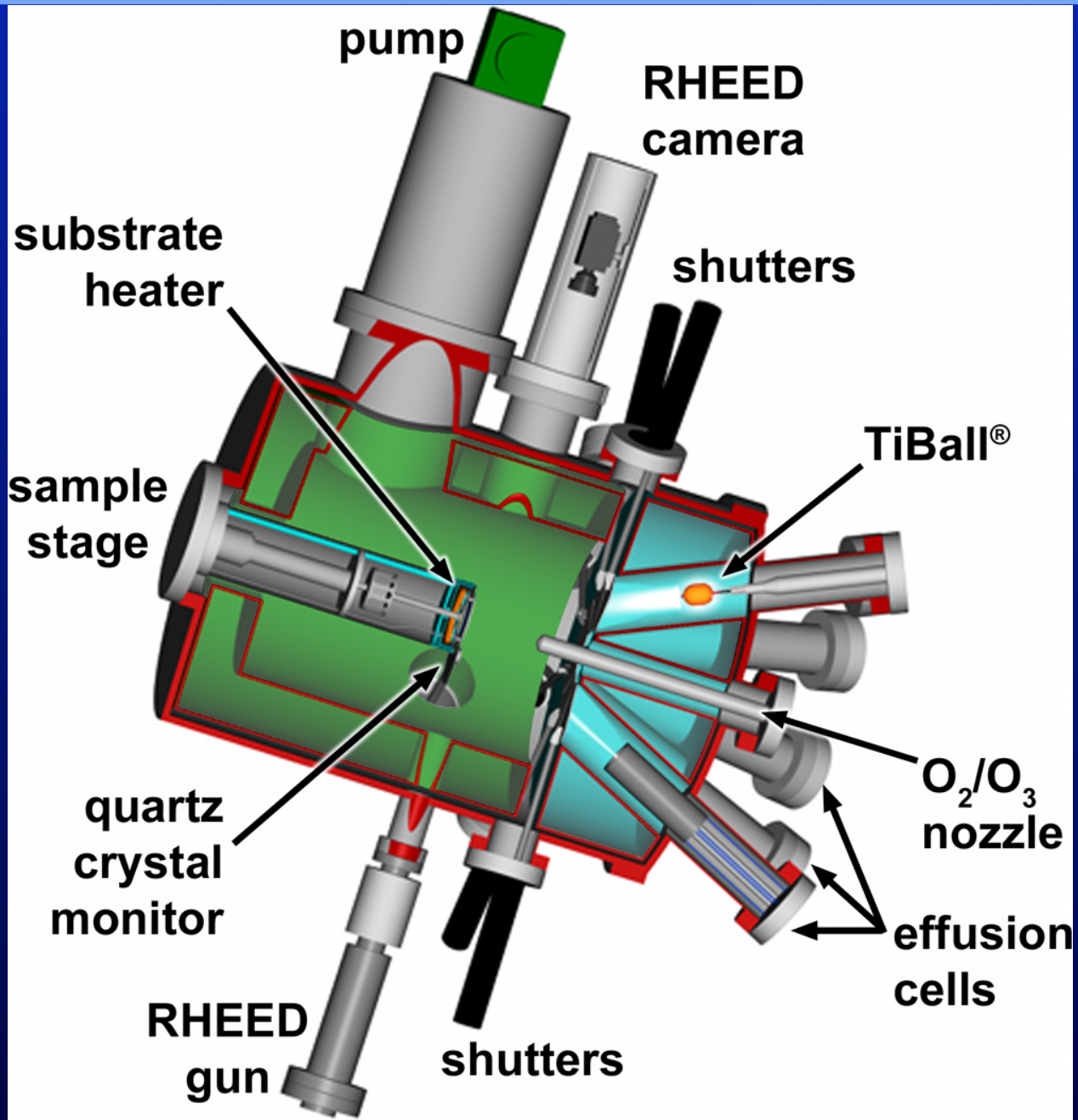

Oxide MBE + ARPES

Collaboration with Kyle Shen (Cornell, Physics)

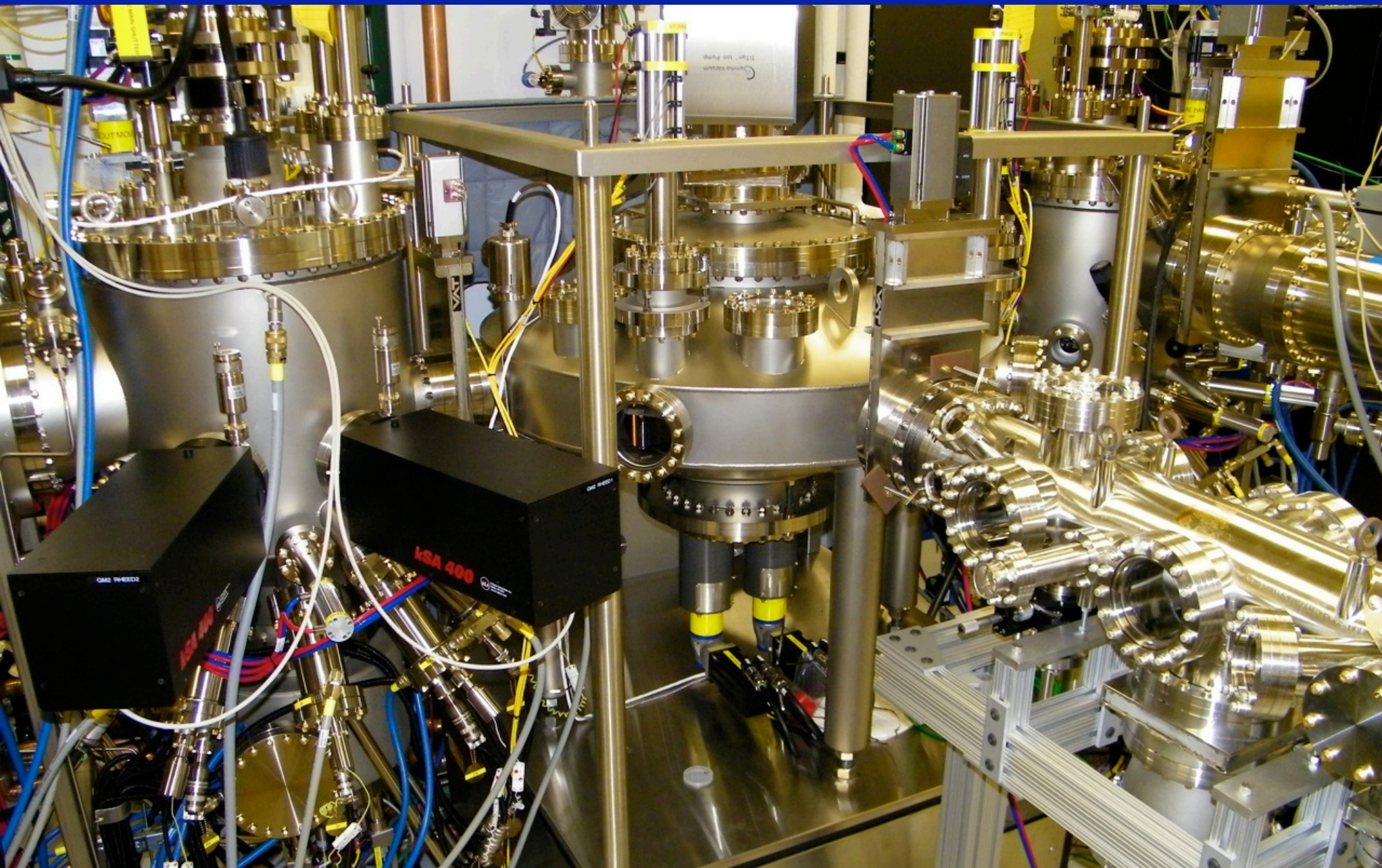

Automated Veeco GEN10 Oxide MBE

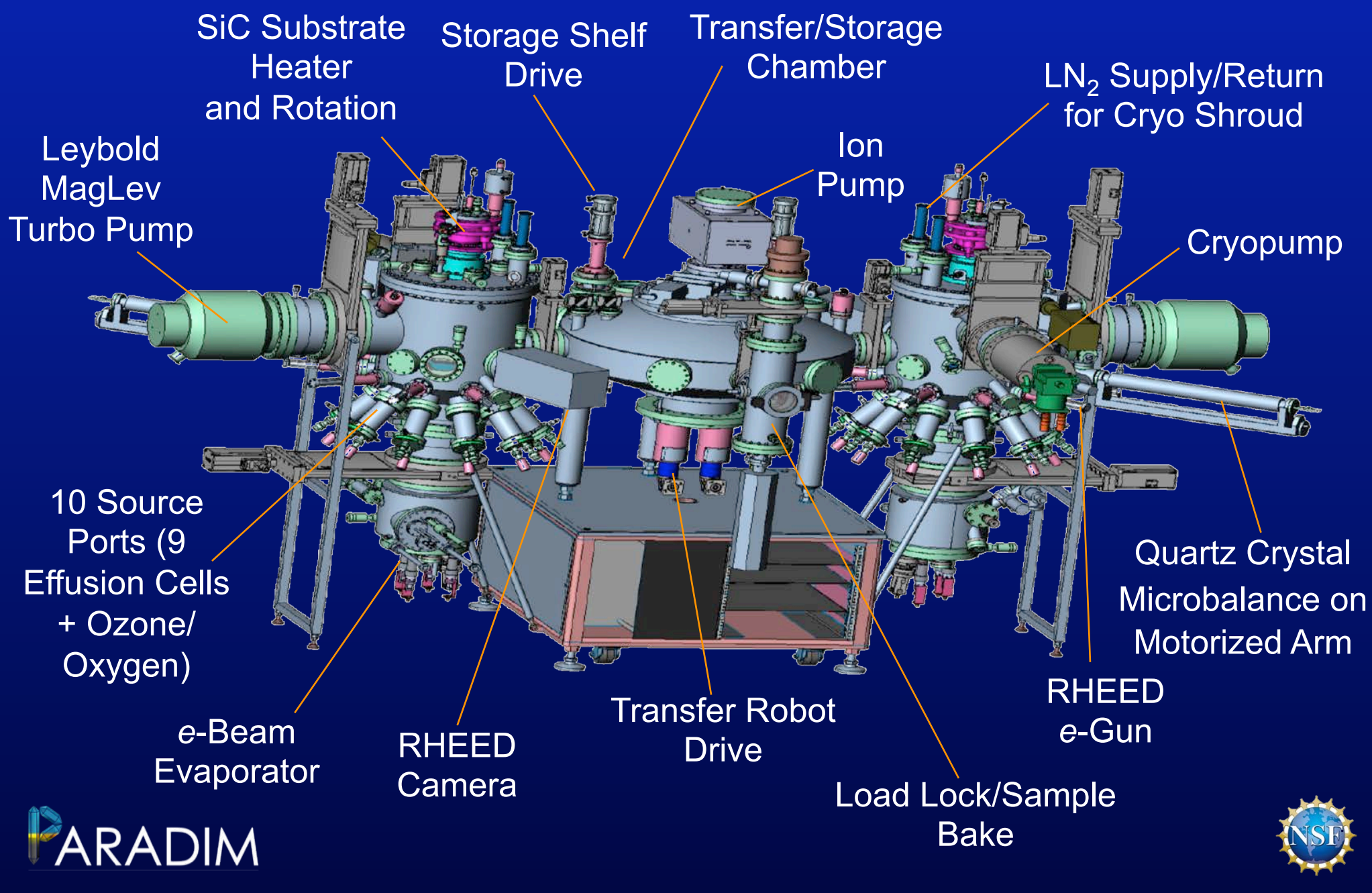

PARADIM

NSF

Oxide MBE at Brookhaven Nat. Lab.

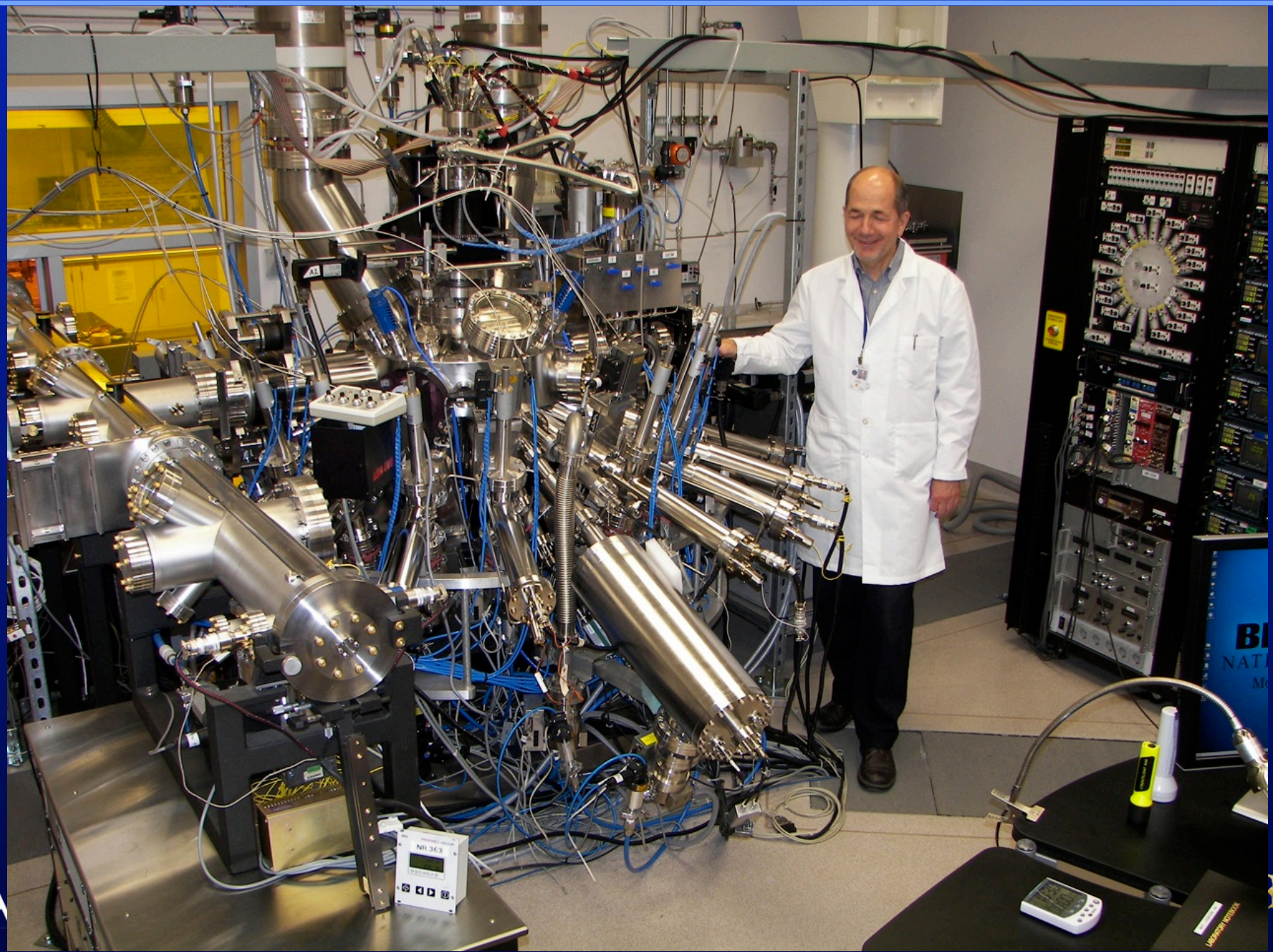

Sources for Oxide MBE

- **Effusion cell**
  (resistively heated thermal evaporators, up to 2000 °C), material in crucible
- **Ti-Ball™ source**
  titanium sphere with resistive heater inside
- **e-gun evaporator**
  for extremely low vapor pressure materials (W, Ru, etc.)

PARADIM

NSF

Ti-Ball™ Source

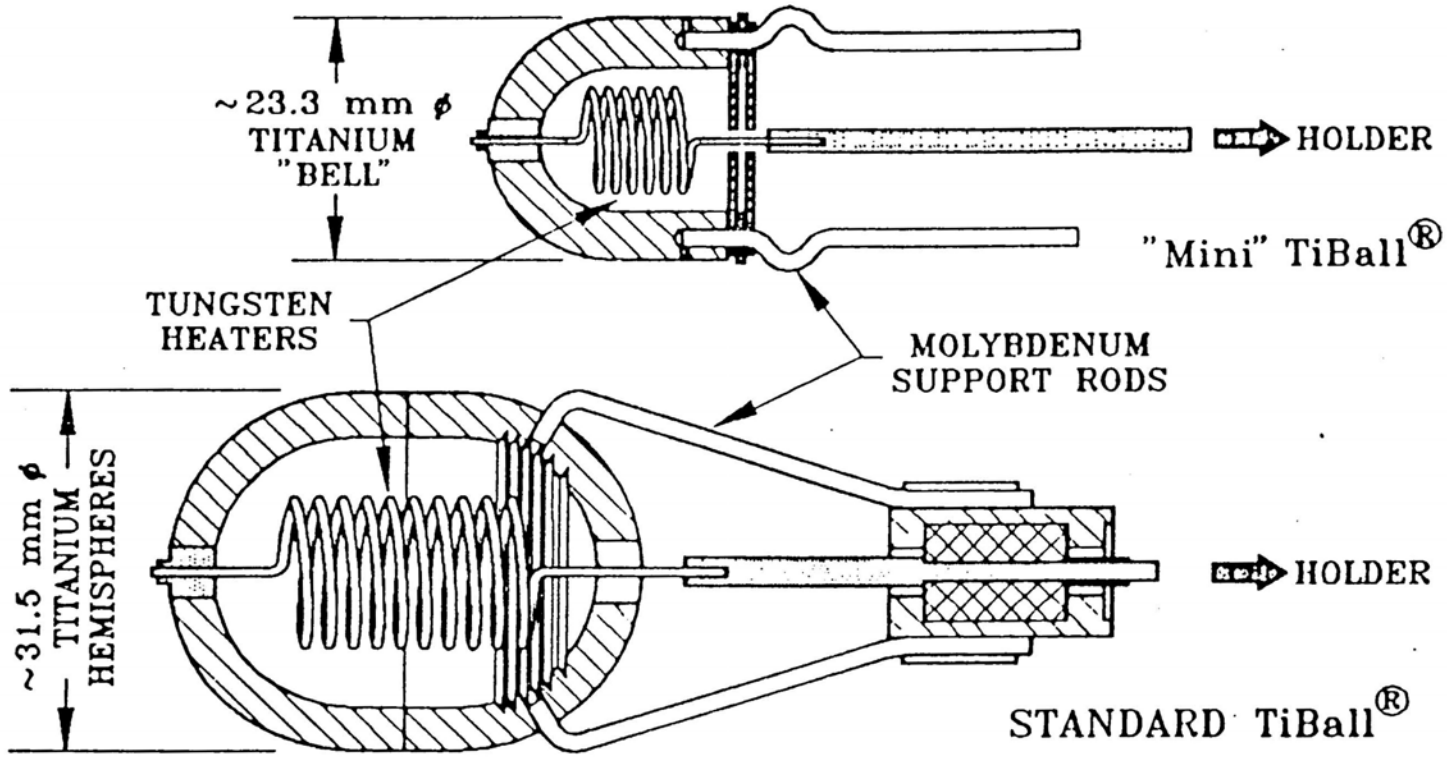

Figure 3.4.4. Two varieties of radiantly heated sublimation sources; the TiBall®, developed by Harra and Snouse[42] and a smaller, radiantly heated source developed by Welch.

CAPTURE PUMPING TECHNOLOGY

An Introduction

KIMO M. WELCH

Brookhaven National Laboratory, Upton, NY, USA

K.M. Welch

Capture Pumping Technology: An Introduction (Pergamon, 1991).

MBE Effusion Cells for Different Temperatures

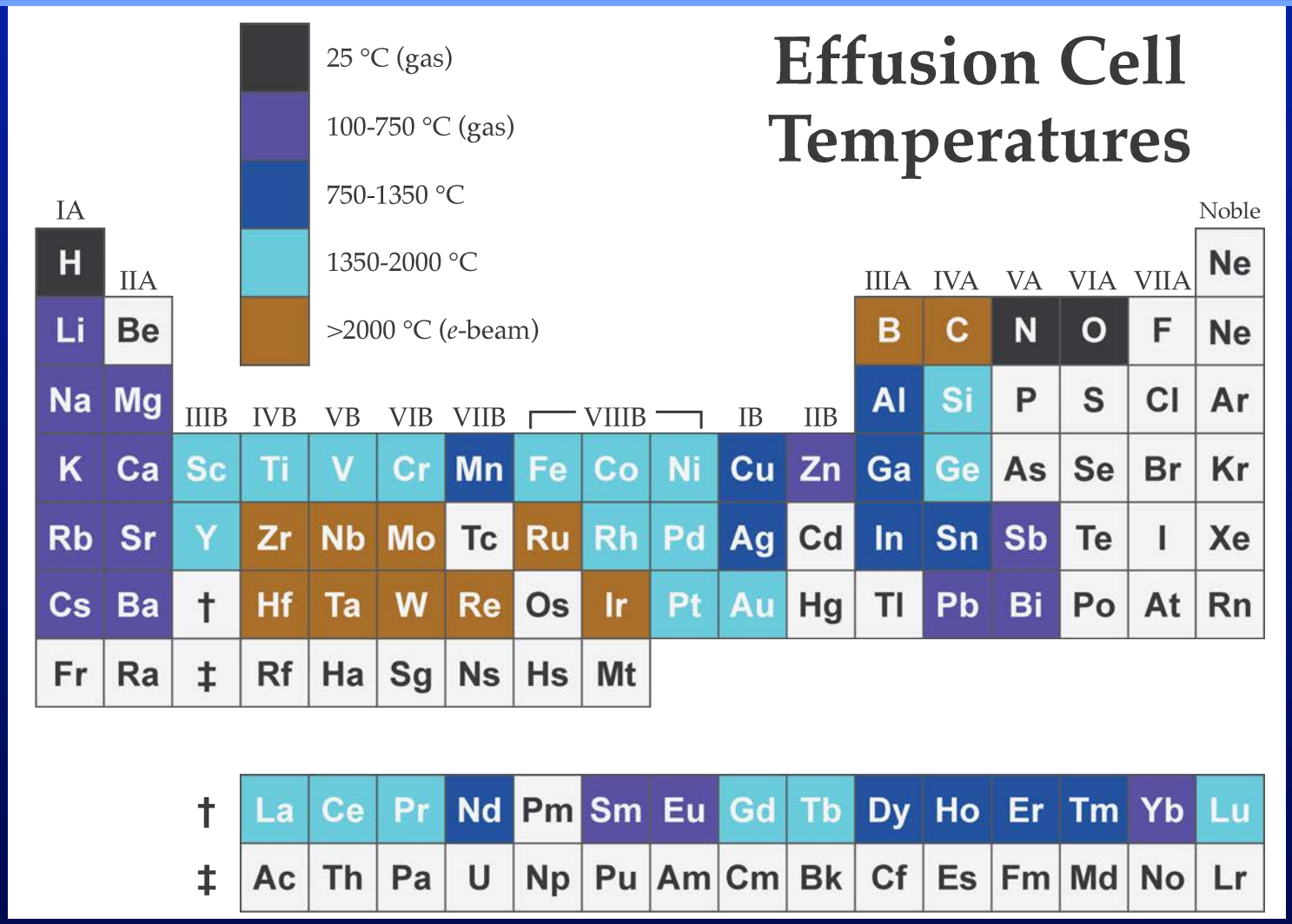

These 62 colored elements are allowed in the PARADIM MBE

MBE Effusion Cells

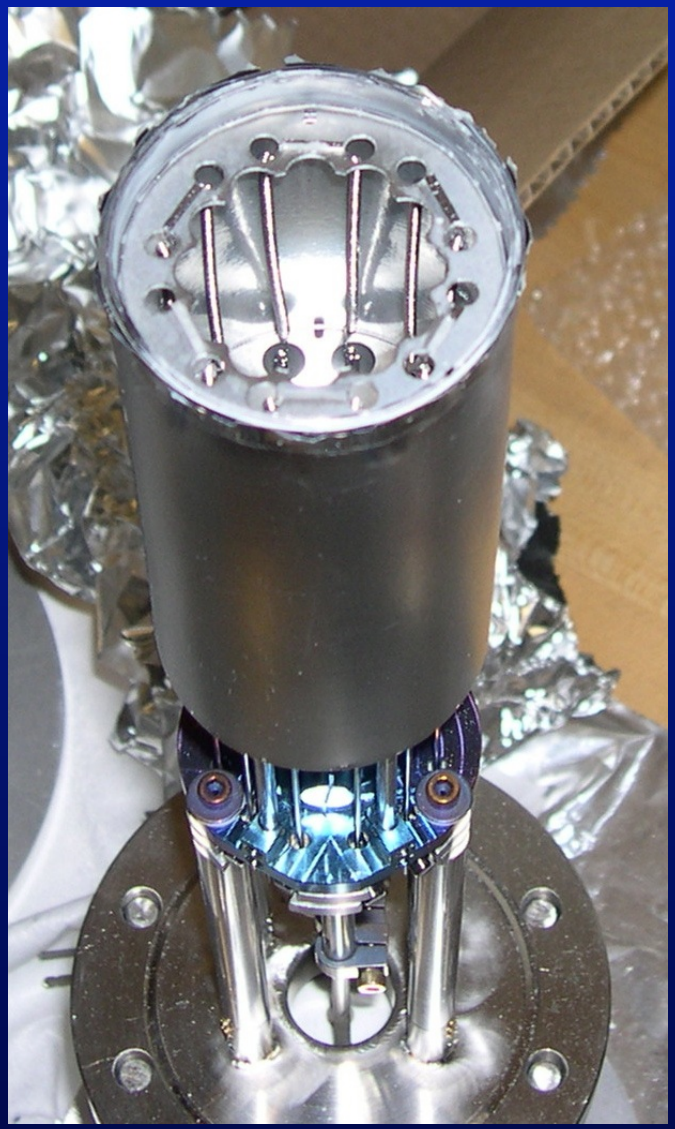

Arrhenius Plot of Vapor Pressure

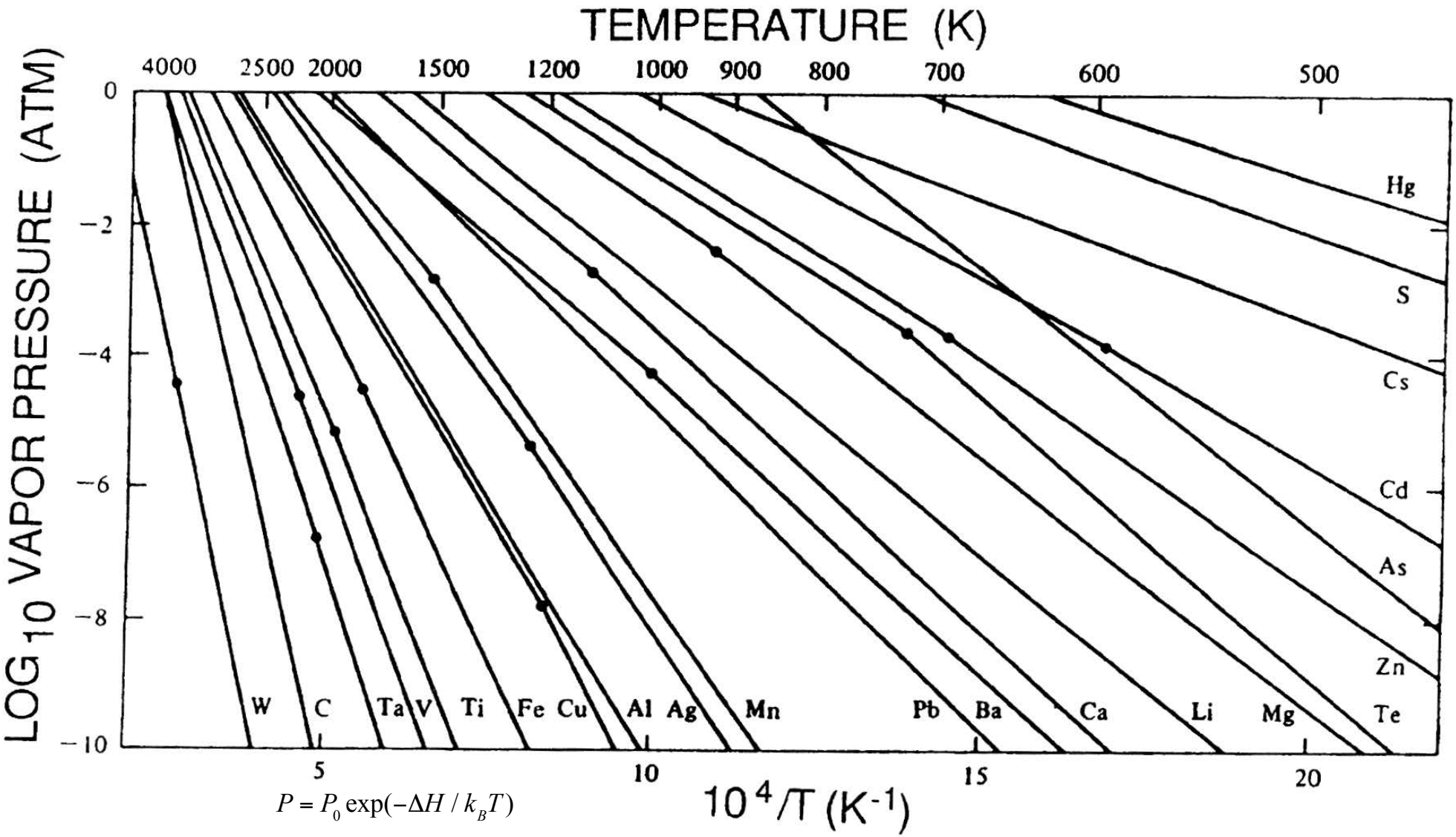

$$P = P_0 \exp(-\Delta H / k_B T)$$

$$\ln P = \ln P_0 - \left(\frac{\Delta H}{k_B}\right) \cdot \left(\frac{1}{T}\right)$$

so plot log(*P*) vs 1/*T*: straight line if ΔH is constant

(note small or no change in slope at melting point)

What Vapor Pressure Needed?

Substrate (growth rate = 0.1 monolayers/s)

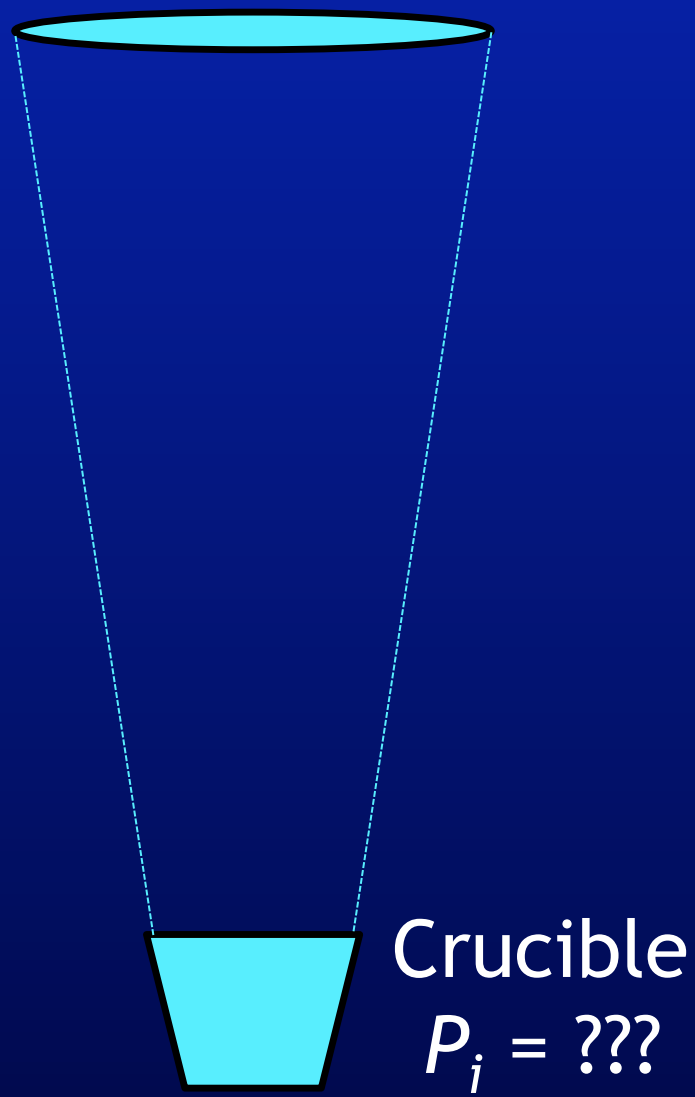

$$\Phi_{Sr} = (0.1)\,\frac{1\ \text{Sr atom}}{(3.905\ \text{Å})^2}\ \text{s}^{-1} = 6.6\times10^{13}\,\frac{\text{atoms}}{\text{cm}^2\ \text{s}}$$

for $SrTiO_3$

From kinetic theory of gases:

$$\Phi = \frac{P}{\sqrt{2\pi\, m\, k_B\, T}}$$

for Sr, m = 87.6 amu and $T \approx 1000$ K

Above is maximum evaporation rate. For free evaporation (as in MBE where wide-mouth (Langmuir) sources are used)

$$\Phi = \frac{\alpha\, P}{\sqrt{2\pi\, m\, k_B\, T}}$$

$\alpha \approx 0.1$ (coefficient of evaporation)

Vapor pressure P_i needs to be larger by ratio of surface area of substrate to surface area of crucible

$$P_i = \frac{\Phi\sqrt{2\pi\, m\, k_B\, T}}{\alpha}(area\ ratio) \approx 10^{-4} - 10^{-3}\ \text{Torr}$$

PARADIM

Crucible for Pb Source

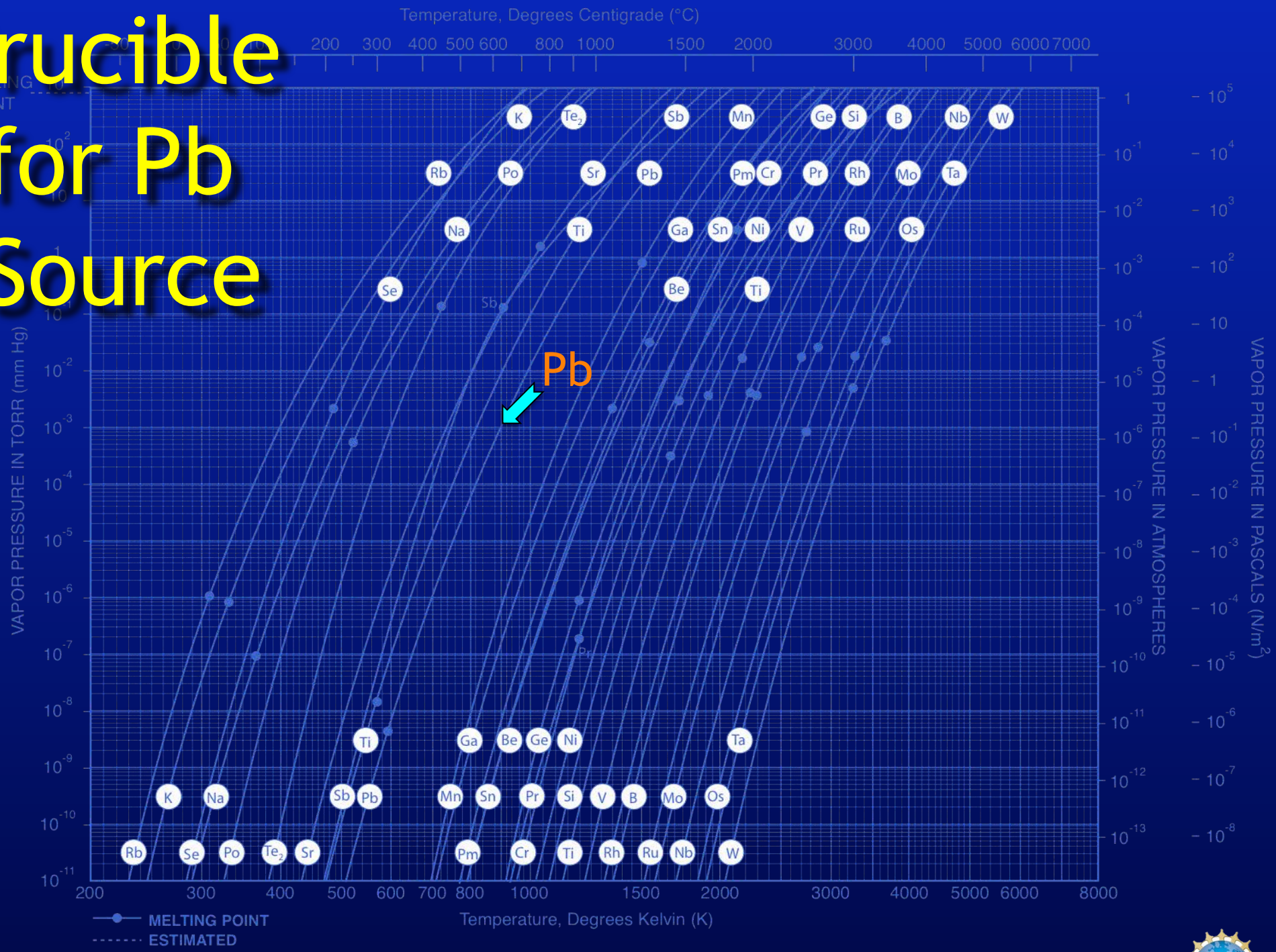

PARADIM

RCA LABORATORIES

Prepared By Richard E. Honig
RADIO CORPORATION OF AMERICA

PRINCETON, N.J.

Ti-Pb Phase Diagram

Binary Alloy Phase Diagrams,
edited by T.B. Massalski (ASM International, 1990).

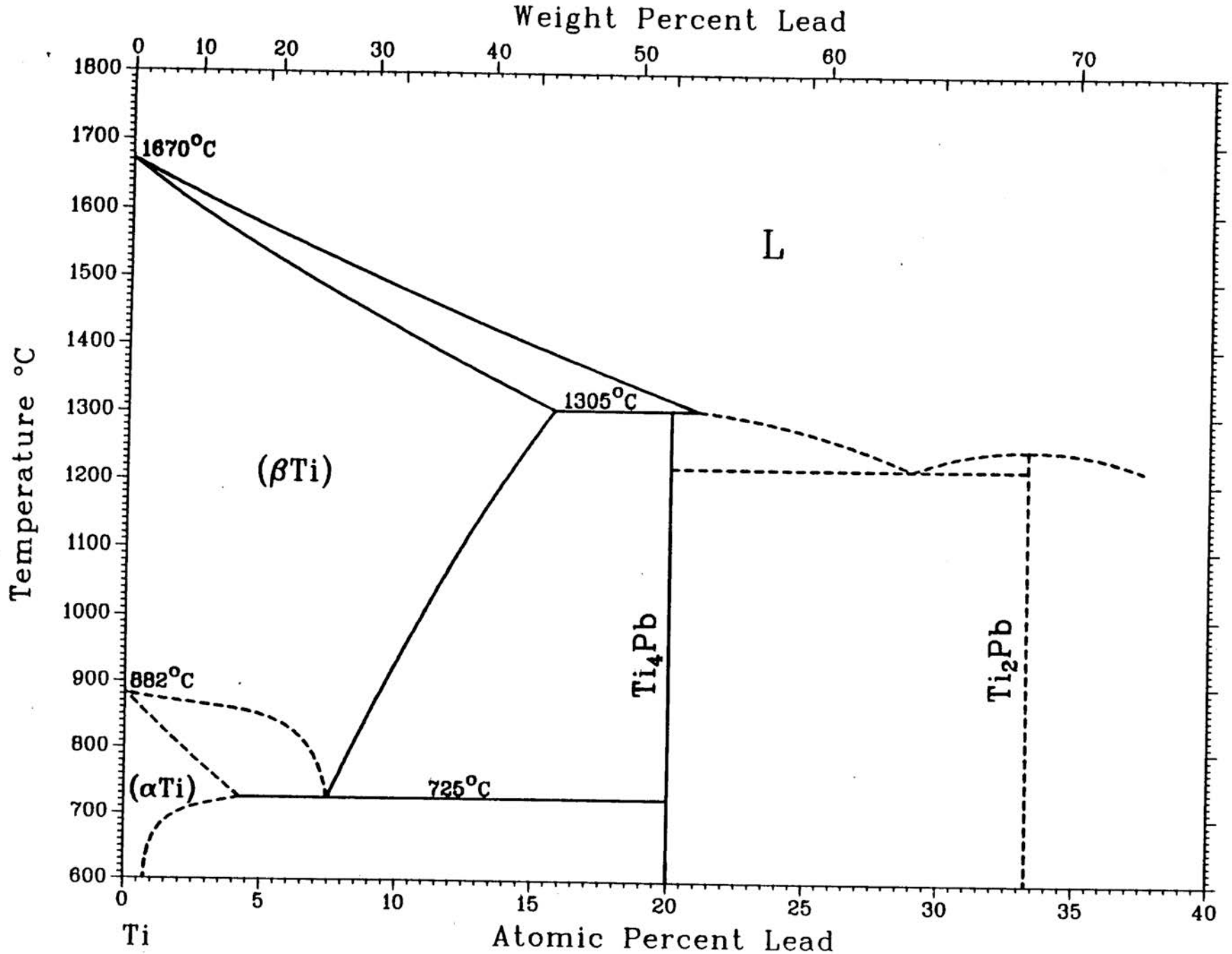

Mo-Pb Phase Diagram

Binary Alloy Phase Diagrams,
edited by T.B. Massalski (ASM International, 1990).

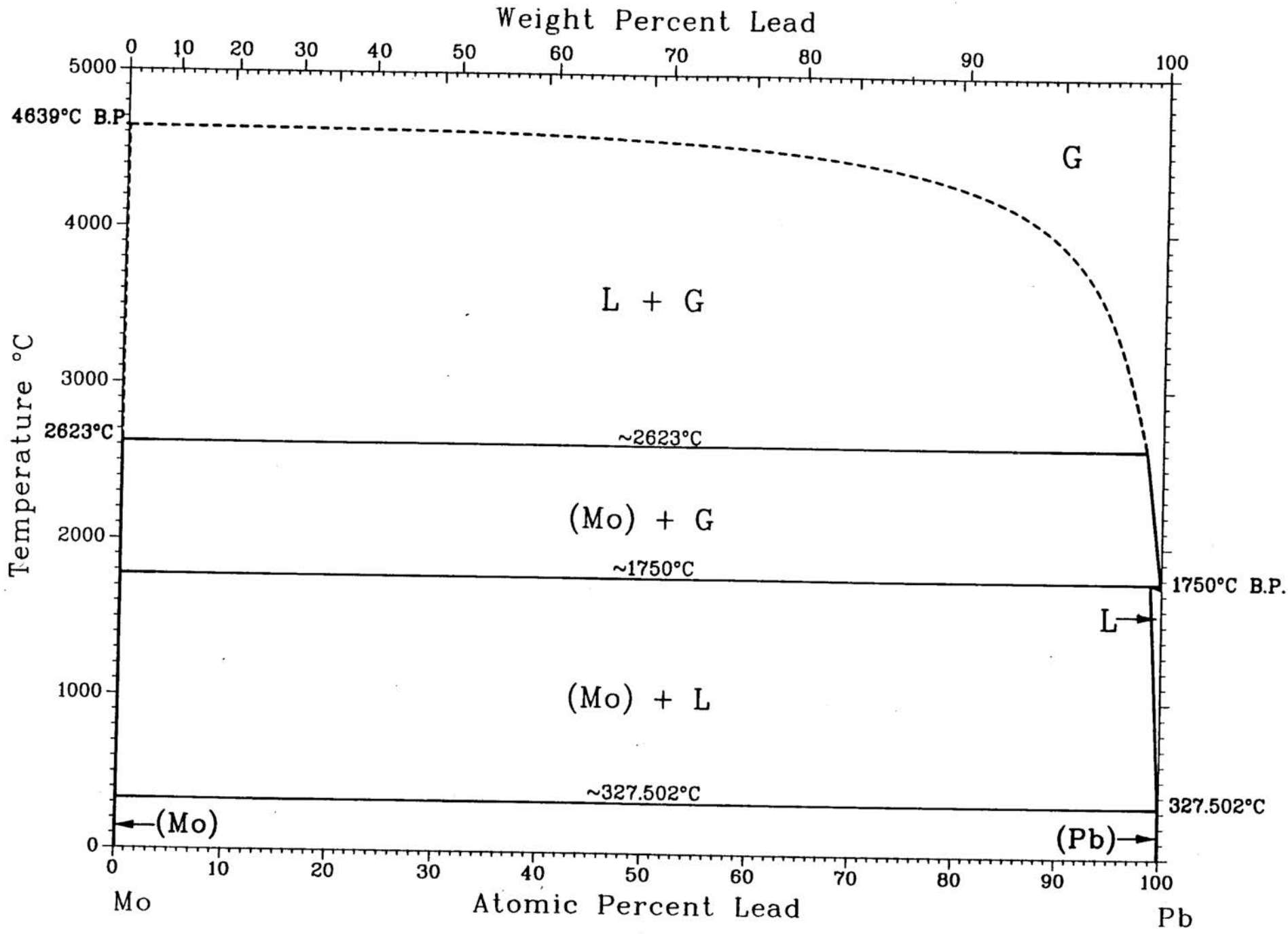

Binary Alloy Phase Diagrams,
edited by T.B. Massalski (ASM International, 1990).

Pb-W (Lead-Tungsten)

S.V. Nagender Naidu and P. Rama Rao

No phase diagram is available for the Pb-W system. The solubility of W in liquid Pb is less than 0.1 at.% W. No intermediate phases exist in the system.

[19Ino] clained to have determined the solidification temperature of alloys containing up to 30 at.% W at 1300 °C; however, no further details are available in this regard. The findings of [19Ino] are not accepted here because there is no confirming evidence in any of the later experimental investigations as to the alloy formation.

Pb-W Crystal Structure Data

Phase	Composition, at.% W	Pearson symbol	Space group	Strukturbericht designation	Prototype
(Pb)	~0	*cF*4	$Fm\bar{3}m$	*A*1	Cu
(W)	~100	*cI*2	$Im\bar{3}m$	*A*2	W

19Ino: S. Inouye, *Mem. Coll. Sci. Kyoto Univ.*, *4*, 43-46 (1919) in German.

To be published in *Phase Diagrams of Binary Tungsten Alloys*, 1991. Complete evaluation contains 1 table and 11 references.

What Crucible to use for Pb?

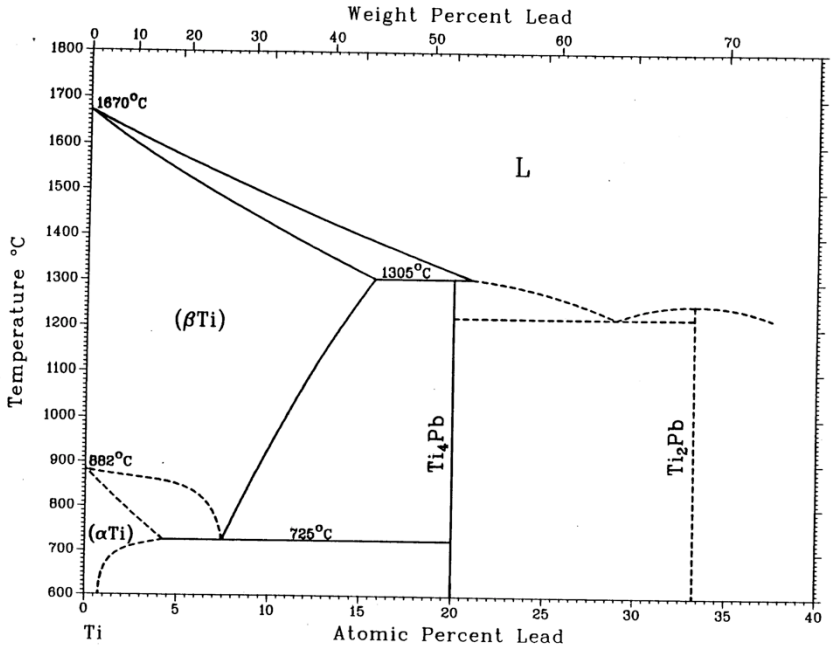

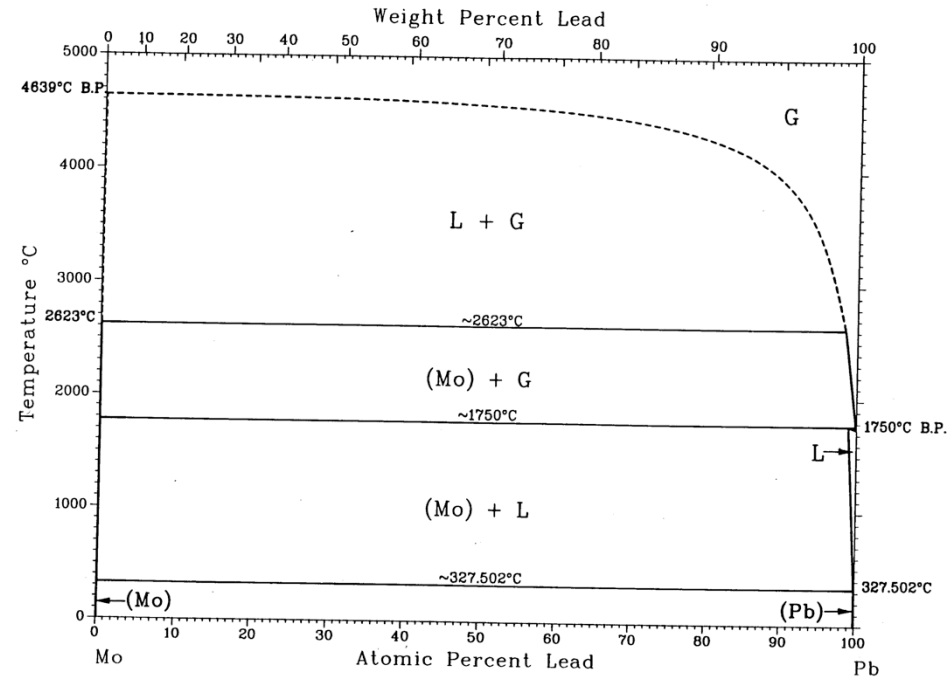

Ti, Mo, or W?

Pb-W (Lead-Tungsten)

S.V. Nagender Naidu and P. Rama Rao

No phase diagram is available for the Pb-W system. The solubility of W in liquid Pb is less than 0.1 at.% W. No intermediate phases exist in the system.

[19Ino] clained to have determined the solidification temperature of alloys containing up to 30 at.% W at 1300 °C; however, no further details are available in this regard. The findings of [19Ino] are not accepted here because there is no confirming evidence in any of the later experimental investigations as to the alloy formation.

Pb-W Crystal Structure Data

Phase	Composition, at.% W	Pearson symbol	Space group	Strukturbericht designation	Prototype
(Pb)	~0	*cF*4	$Fm\bar{3}m$	*A*1	Cu
(W)	~100	*cI*2	$Im\bar{3}m$	*A*2	W

19Ino: S. Inouye, *Mem. Coll. Sci. Kyoto Univ.*, *4*, 43-46 (1919) in German.

To be published in *Phase Diagrams of Binary Tungsten Alloys*, 1991. Complete evaluation contains 1 table and 11 references.

PARADIM

NSF

Material	Symbol	MP (° C)	S/D	g/cm³	Temp. (° C) for Given Vap. Press. (Torr) 10^{-8}	10^{-6}	10^{-4}	Evaporation Techniques: E-Beam	Thermal Sources: Boat	Coil	Basket	Crucible	Sputter	Comments
Kanthal	FeCrAl	—	—	7.1	—	—	—	—	W	W	W	—	DC, RF	—
Lanthanum	La	921	—	6.15	990	1,212	1,388	Ex	W, Ta	—	—	Al_2O_3	RF	Films will burn in air if scraped
Lanthanum Boride	LaB_6	2,210	D	2.61	—	—	—	G	—	—	—	—	RF	—
Lanthanum Bromide	$LaBr_3$	783	—	5.06	—	—	—	—	—	—	Ta	—	RF	n=1.94. Hygroscopic
Lanthanum Fluoride	LaF_3	1,490	S	~6.0	—	—	900	G	Ta, Mo	—	Ta	—	RF	No decomposition. n ~1.6
Lanthanum Oxide	La_2O_3	2,307	—	6.51	—	—	1,400	G	W, Ta	—	—	—	RF	Loses oxygen. n~1.73
Lead	Pb	328	—	11.34	342	427	497	Ex	W, Mo	W	W, Ta	Al2O3, Q	DC,	RF Toxic
Lead Bromide	$PbBr_2$	373	—	6.66	—	—	~300	—	—	—	—	—	—	—
Lead Chloride	$PbCl_2$	501	—	5.85	—	—	~325	—	Pt	—	—	Al_2O_3	RF	Little decomposition
Lead Fluoride	PbF_2	855	S	8.24	—	—	~400	—	W, Pt, Mo	—	—	BeO	RF	n = 1.75
Lead Iodide	PbI_2	402	—	6.16	—	—	~500	—	Pt	—	—	Q	—	—
Lead Oxide	PbO	886	—	9.53	—	—	~550	—	Pt	—	—	Q, Al_2O_3	RF-R	No decomposition. n ~2.6
Lead Selenide	PbSe	1,065	S	8.10	—	—	~500	—	W, Mo	—	W	Gr, Al_2O_3	RF	—
Lead Stannate	$PbSnO_3$	1,115	—	8.1	670	780	905	P	Pt	—	Pt	Al_2O_3	RF	Disproportionates
Lead Sulfide	PbS	1,114	S	7.5	—	—	500	—	W	—	W, Mo	Q, Al_2O_3	RF	Little decomposition. n = 3.92
Lead Telluride	PbTe	917	—	8.16	780	910	1,050	—	Mo, Pt, Ta	—	—	Al_2O_3, Gr	RF	Vapors toxic. Deposits aretellurium rich. Sputtering preferred or co-evaporate from two sources
Lead Titanate	$PbTiO_3$	—	—	7.52	—	—	—	—	Ta	—	—	—	RF	—
Lithium	Li	181	—	0.53	227	307	407	G	Ta, SS	—	—	Al_2O_3, BeO	—	Metal reacts quickly in air
Lithium Bromide	LiBr	550	—	3.46	—	—	~500	—	Ni	—	—	—	RF	n = 1.78
Lithium Chloride	LiCl	605	—	2.07	—	—	400	—	Ni	—	—	—	RF	Preheat gently to outgas. n = 1.66
Lithium Fluoride	LiF	845	—	2.64	875	1,020	1,180	G	Ni, Ta, Mo, W	—	—	Al_2O_3	RF	Rate control important for optical films. Preheat gently to outgas. n = 1.39
Lithium Iodide	LiI	449	—	4.08	—	—	400	—	Mo, W	—	—	—	RF	n = 1.96
Lithium Oxide	Li_2O	>1,700	—	2.01	—	—	850	—	Pt, Ir	—	—	—	RF	n = 1.64
Lutetium	Lu	1,663	—	9.84	—	—	1,300	Ex	Ta	—	—	Al_2O_3	RF, DC	—
Lutetium Oxide	Lu_2O_3	—	—	9.42	—	—	1,400	—	Ir	—	—	—	RF	Decomposes

Key of Symbols: * influenced by composition; ** Cr-plated rod or strip; ***all metals alumina coated; **C** = carbon; **Gr** = graphite; **Q** = quartz; **Incl** = Inconel; **VC** = vitreous carbon; **SS** = stainless steel; **Ex** = excellent; **G** = good; **F** = fair; **P** = poor; **S** = sublimes; **D** = decomposes; **RF** = RF sputtering is effective; **RF-R** = reactive RF sputter is effective; **DC** = DC sputtering is effective; **DC-R** = reactive DC sputtering is effective

Kurt J. Lesker, Co. Catalog

Crucible for V Source

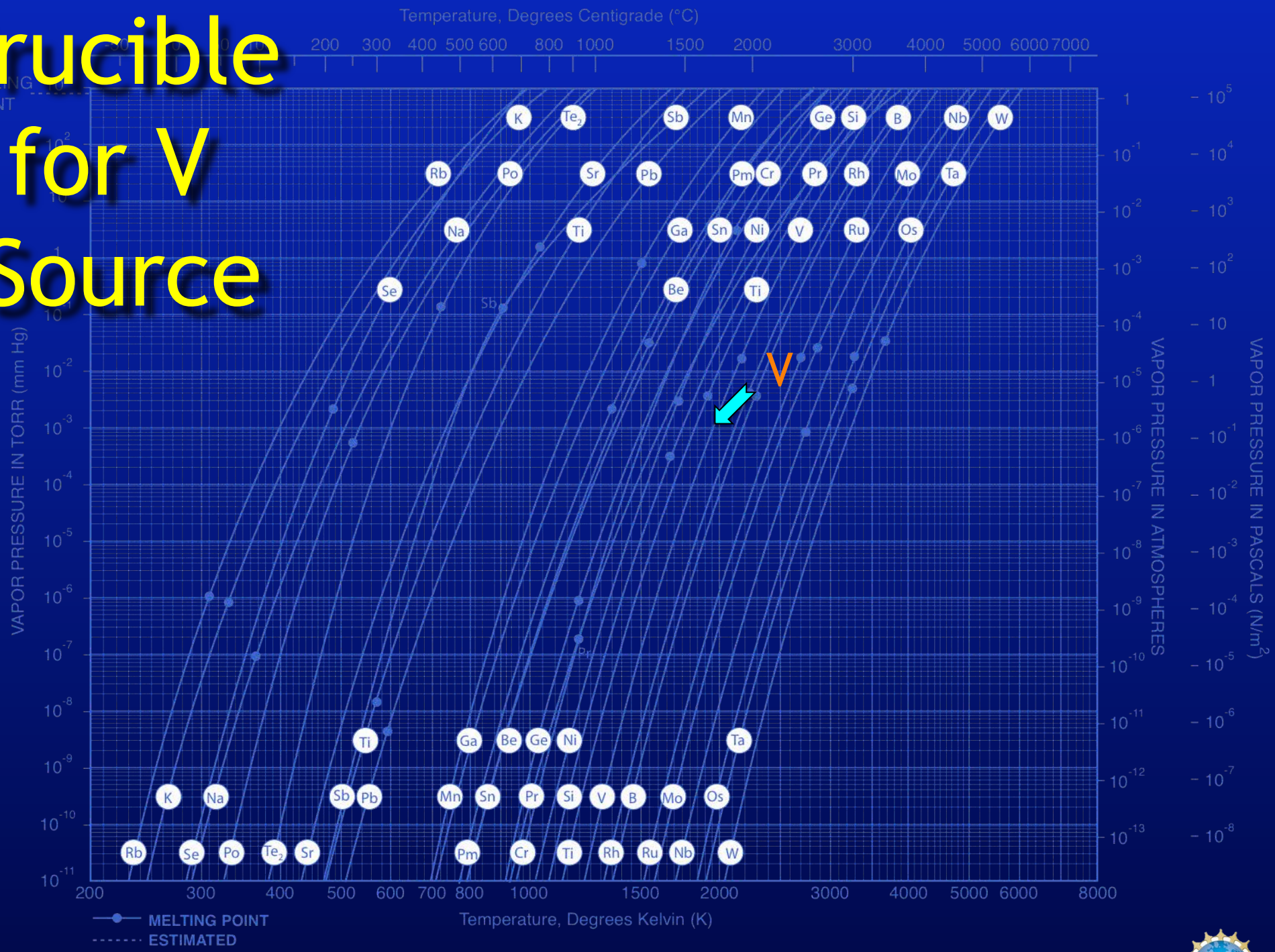

PARADIM

RCA LABORATORIES

Prepared By Richard E. Honig
RADIO CORPORATION OF AMERICA

PRINCETON, N.J.

What Crucible to use for V?

Desk Handbook: Phase Diagrams for Binary Alloys, edited by H. Okamoto (ASM International, 2000).

C, Sr, Ti, W?

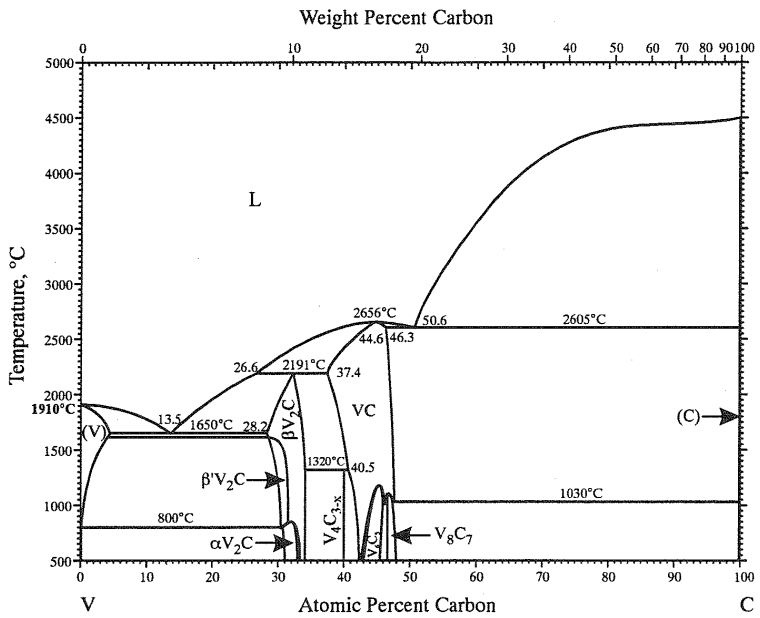

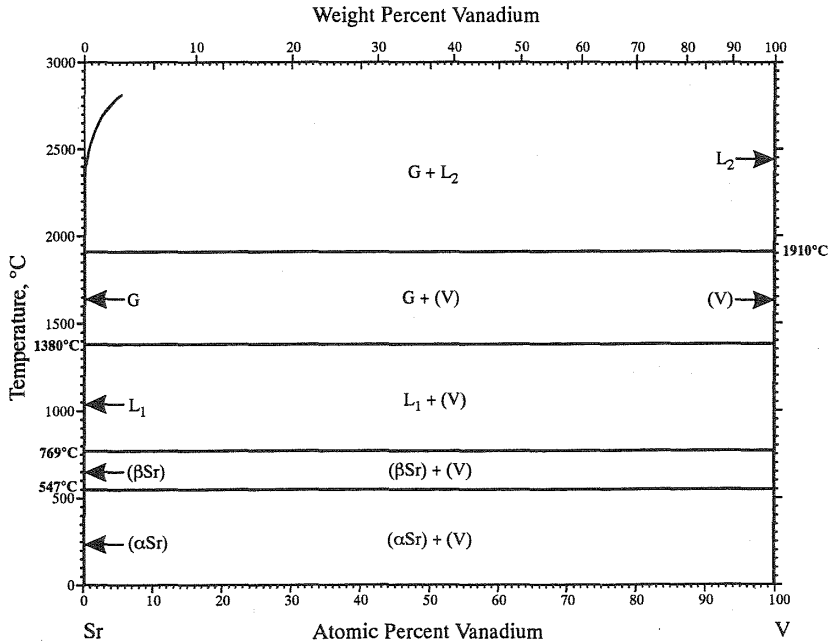

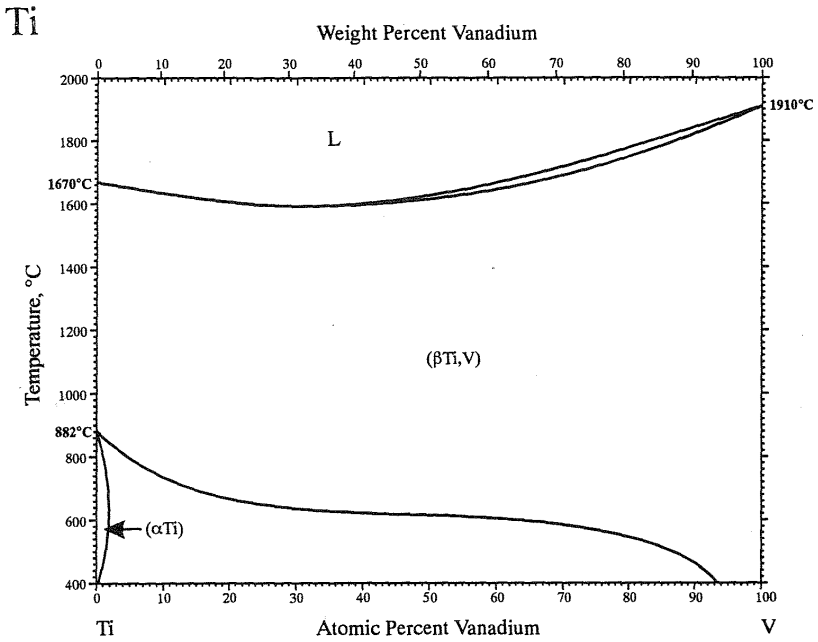

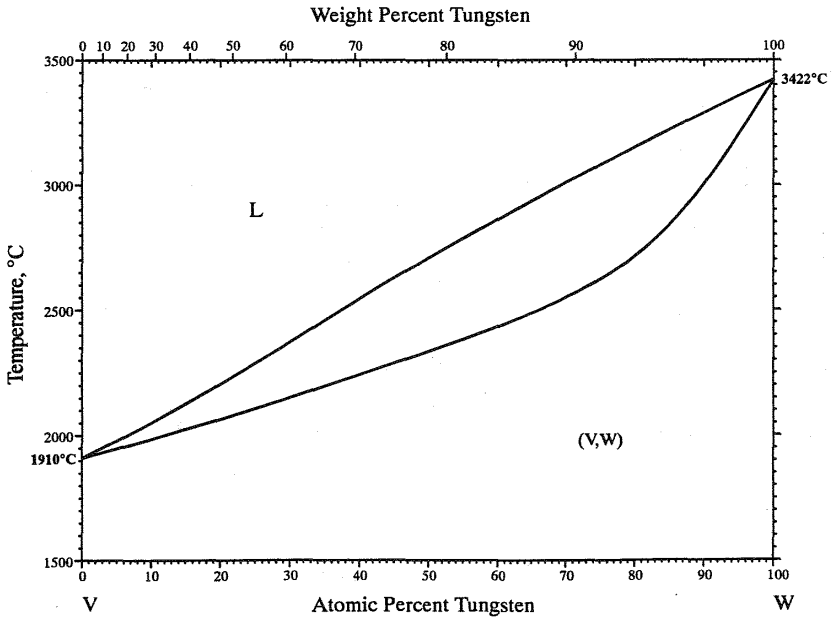

Material	Symbol	MP (° C)	S/D	g/cm³	Temp. (° C) for Given Vap. Press. (Torr) 10^{-8}	10^{-6}	10^{-4}	Evaporation Techniques: E-Beam	Thermal Sources: Boat	Coil	Basket	Crucible	Sputter	Comments
Thulium	Tm	1,545	S	9.32	461	554	680	G	Ta	—	—	Al_2O_3	DC	—
Thulium Oxide	Tm_2O_3	—	—	8.90	—	—	1,500	—	Ir	—	—	—	RF	Decomposes
Tin	Sn	232	—	7.28	682	807	997	Ex	Mo	W	W	Al_2O_3	DC, RF	Wets molybdenum Use tantalum liner in E-beam guns
Tin Oxide	SnO_2	1,630	S	6.95	—	—	~1,000	Ex	W	W	W	Q, Al_2O_3	RF, RF-R	Films from tungsten are oxygen deficient, oxidize in air. n = 2.0
Tin Selenide	SnSe	861	—	6.18	—	—	~400	G	—	—	—	Q	RF	—
Tin Sulfide	SnS	882	—	5.22	—	—	~450	—	—	—	—	Q	RF	—
Tin Telluride	SnTe	780	D	6.48	—	—	~450	—	—	—	—	Q	RF	—
Titanium	Ti	1,660	—	4.5	1,067	1,235	1,453	Ex	W	—	—	TiC	DC, RF	Alloys with refractory metals; evolves gas on first heating
Titanium Boride	TiB_2	2,900	—	4.50	—	—	—	P	—	—	—	—	RF, DC	—
Titanium Carbide	TiC	3,140	—	4.93	—	—	~2,300	—	—	—	—	—	RF, DC	—
Titanium Nitride	TiN	2,930	—	5.22	—	—	—	G	Mo	—	—	—	RF, RF-R, DC	Sputtering preferred. Decomposes with thermal evaporation
Titanium (II) Oxide	TiO	1,750	—	4.93	—	—	~1,500	G	W, Mo	—	—	VC	RF	Preheat gently to outgas. n = 2.2
Titanium (III) Oxide	Ti_2O_3	2,130	D	4.6	—	—	—	G	W	—	—	—	RF	Decomposes
Titanium (IV) Oxide	TiO_2	1,830	—	4.26	—	—	~1,300	F	W, Mo	—	W	—	RF, RF-R	Suboxide, must be reoxidized to rutile. Tantalum reduces TiO_2 to TiO and titanium. n = 2.616, 2.903
Tungsten	W	3,410	—	19.35	2,117	2,407	2,757	G	—	—	—	—	RF, DC	Forms volatile oxides. Films hard and adherent
Tungsten Boride	WB_2	~2,900	—	10.77	—	—	—	P	—	—	—	—	RF	—
Tungsten Carbide	W_2C	2,860	—	17.15	1,480	1,720	2,120	Ex	C	—	—	—	RF, DC	—
Tungsten Disulfide	WS_2	1,250	D	7.5	—	—	—	—	—	—	—	—	RF	—
Tungsten Oxide	WO_3	1,473	S	7.16	—	—	980	G	W, Pt	—	—	—	RF-R	Preheat gently to outgas. Tungsten reduces oxide slightly. n = 1.68
Tungsten Selenide	WSe_2	—	—	9.0	—	—	—	—	—	—	—	—	RF	—
Tungsten Silicide	WSi2	>900	—	9.4	—	—	—	—	—	—	—	—	RF, DC	—
Tungsten Telluride	WTe_3	—	—	9.49	—	—	—	—	—	—	—	Q	RF	—
Uranium	U	1,132	—	19.05	1,132	1,327	1,582	G	Mo, W	W	W	—	—	Films oxidize
Uranium Carbide	UC_2	2,350	—	11.28	—	—	2,100	—	—	—	—	C	RF	Decomposes
Uranium Fluoride	UF_4	960	—	6.70	—	—	300	—	Ni	—	—	—	RF	—
Uranium (III) Oxide	U_2O_3	1,300	D	8.30	—	—	—	—	W	—	W	—	RF-R	Disproportionates at 1,300° C to UO_2
Uranium (IV) Oxide	UO_2	2,878	—	10.96	—	—	—	—	W	—	W	—	RF	Tantalum causes decomposition
Uranium Phosphide	UP_2	—	—	8.57	—	—	1,200	—	Ta	—	—	—	RF	Decomposes
Uranium (II) Sulfide	US	>2,000	—	10.87	—	—	—	—	—	—	—	—	—	—
Uranium (IV) Sulfide	US_2	>1,100	—	7.96	—	—	—	—	W	—	—	—	RF	Slight decomposition
Vanadium	V	1,890	—	5.96	1,162	1,332	1,547	Ex	W, Mo	—	—	—	DC, RF	Wets molybdenum. E-beam-evaporated films preferred. n = 3.03
Vanadium Boride	VB_2	2,400	—	5.10	—	—	—	—	—	—	—	—	RF, DC	—
Vanadium Carbide	VC	2,810	—	5.77	—	—	~1,800	—	—	—	—	—	RF, DC	—
Vanadium Nitride	VN	2,320	—	6.13	—	—	—	—	—	—	—	—	RF, RF-R, DC	—
Vanadium (IV) Oxide	VO_2	1,967	S	4.34	—	—	~575	—	—	—	—	—	RF, RF-R	Sputtering preferred.
Vanadium (V) Oxide	V_2O_5	690	D	3.36	—	—	~500	—	—	—	—	Q	RF	n = 1.46, 1.52, 1.76
Vanadium Silicide	VSi_2	1,700	—	4.42	—	—	—	—	—	—	—	—	RF	—
Ytterbium	Yb	819	S	6.96	520	590	690	G	Ta	—	—	—	DC, RF	—
Ytterbium Fluoride	YbF_3	1,157	—	—	—	—	~800	—	Mo	—	—	—	RF	—
Ytterbium Oxide	Yb_2O_3	2,346	S	9.17	—	—	~1,500	—	Ir	—	—	—	RF, RF-R	Loses oxygen

Key of Symbols: * influenced by composition; ** Cr-plated rod or strip; ***all metals alumina coated; **C** = carbon; **Gr** = graphite; **Q** = quartz; **Incl** = Inconel; **VC** = vitreous carbon; **SS** = stainless steel; **Ex** = excellent; **G** = good; **F** = fair; **P** = poor; **S** = sublimes; **D** = decomposes; **RF** = RF sputtering is effective; **RF-R** = reactive RF sputter is effective; **DC** = DC sputtering is effective; **DC-R** = reactive DC sputtering is effective

Kurt J. Lesker, Co. Catalog

Advanced Ceramics
CORPORATION

Reactions with Boron Nitride (PBN)

Expected Reactions as calculated from free energies

H 1																	He 2
Li 3	Be 4											B 5	C 6	N 7	O 8	F 9	Ne 10
Na 11	Mg 12											Al 13	Si 14	P 15	S 16	Cl 17	Ar 18
K 19	Ca 20	Sc 21	Ti 22	V 23	Cr 24	Mn 25	Fe 26	Co 27	Ni 28	Cu 29	Zn 30	Ga 31	Ge 32	As 33	Se 34	Br 35	Kr 36
Rb 37	Sr 38	Y 39	Zr 40	Nb 41	Mo 42	Tc 43	Ru 44	Rh 45	Pd 46	Ag 47	Cd 48	In 49	Sn 50	Sb 51	Te 52	I 53	Xe 54
Cs 55	Ba 56	La 57	Hf 72	Ta 73	W 74	Re 75	Os 76	Ir 77	Pt 78	Au 79	Hg 80	Ti 81	Pb 82	Bi 83	Po 84	At 85	Rn 86
Fr 87	Ra 88	Ac 89	103														

Ce 58	Pr 59	Nd 60	Pm 61	Sm 62	Eu 63	Gd 64	Tb 65	Dy 66	Ho 67	Er 68	Tm 69	Yb 70	Lu 71
Th 90	Pa 91	U 92	Np 93	Pu 94	Am 95	Cm 96	Bk 97	Cf 98	Es 99	Fm 100	Md 101	102	Lw 103

Reactions with Carbon (PG)

Expected Reactions as calculated from free energies

H 1																	He 2
Li 3	Be 4											B 5	C 6	N 7	O 8	F 9	Ne 10
Na 11	Mg 12											Al 13	Si 14	P 15	S 16	Cl 17	Ar 18
K 19	Ca 20	Sc 21	Ti 22	V 23	Cr 24	Mn 25	Fe 26	Co 27	Ni 28	Cu 29	Zn 30	Ga 31	Ge 32	As 33	Se 34	Br 35	Kr 36
Rb 37	Sr 38	Y 39	Zr 40	Nb 41	Mo 42	Tc 43	Ru 44	Rh 45	Pd 46	Ag 47	Cd 48	In 49	Sn 50	Sb 51	Te 52	I 53	Xe 54
Cs 55	Ba 56	La 57	Hf 72	Ta 73	W 74	Re 75	Os 76	Ir 77	Pt 78	Au 79	Hg 80	Ti 81	Pb 82	Bi 83	Po 84	At 85	Rn 86
Fr 87	Ra 88	Ac 89	103														

Ce 58	Pr 59	Nd 60	Pm 61	Sm 62	Eu 63	Gd 64	Tb 65	Dy 66	Ho 67	Er 68	Tm 69	Yb 70	Lu 71
Th 90	Pa 91	U 92	Np 93	Pu 94	Am 95	Cm 96	Bk 97	Cf 98	Es 99	Fm 100	Md 101	102	Lw 103

Reactions with NbC & TaC

Expected Reactions as calculated from free energies

H 1																	He 2
Li 3	Be 4											B 5	C 6	N 7	O 8	F 9	Ne 10
Na 11	Mg 12											Al 13	Si 14	P 15	S 16	Cl 17	Ar 18
K 19	Ca 20	Sc 21	Ti 22	V 23	Cr 24	Mn 25	Fe 26	Co 27	Ni 28	Cu 29	Zn 30	Ga 31	Ge 32	As 33	Se 34	Br 35	Kr 36
Rb 37	Sr 38	Y 39	Zr 40	Nb 41	Mo 42	Tc 43	Ru 44	Rh 45	Pd 46	Ag 47	Cd 48	In 49	Sn 50	Sb 51	Te 52	I 53	Xe 54
Cs 55	Ba 56	La 57	Hf 72	Ta 73	W 74	Re 75	Os 76	Ir 77	Pt 78	Au 79	Hg 80	Ti 81	Pb 82	Bi 83	Po 84	At 85	Rn 86
Fr 87	Ra 88	Ac 89	103														

Ce 58	Pr 59	Nd 60	Pm 61	Sm 62	Eu 63	Gd 64	Tb 65	Dy 66	Ho 67	Er 68	Tm 69	Yb 70	Lu 71
Th 90	Pa 91	U 92	Np 93	Pu 94	Am 95	Cm 96	Bk 97	Cf 98	Es 99	Fm 100	Md 101	102	Lw 103

Reactions with SiC

Expected Reactions as calculated from free energies

H 1																	He 2
Li 3	Be 4											B 5	C 6	N 7	O 8	F 9	Ne 10
Na 11	Mg 12											Al 13	Si 14	P 15	S 16	Cl 17	Ar 18
K 19	Ca 20	Sc 21	Ti 22	V 23	Cr 24	Mn 25	Fe 26	Co 27	Ni 28	Cu 29	Zn 30	Ga 31	Ge 32	As 33	Se 34	Br 35	Kr 36
Rb 37	Sr 38	Y 39	Zr 40	Nb 41	Mo 42	Tc 43	Ru 44	Rh 45	Pd 46	Ag 47	Cd 48	In 49	Sn 50	Sb 51	Te 52	I 53	Xe 54
Cs 55	Ba 56	La 57	Hf 72	Ta 73	W 74	Re 75	Os 76	Ir 77	Pt 78	Au 79	Hg 80	Ti 81	Pb 82	Bi 83	Po 84	At 85	Rn 86
Fr 87	Ra 88	Ac 89	103														

Ce 58	Pr 59	Nd 60	Pm 61	Sm 62	Eu 63	Gd 64	Tb 65	Dy 66	Ho 67	Er 68	Tm 69	Yb 70	Lu 71
Th 90	Pa 91	U 92	Np 93	Pu 94	Am 95	Cm 96	Bk 97	Cf 98	Es 99	Fm 100	Md 101	102	Lw 103

Advanced Ceramics Corporation • 11907 Madison Avenue • Cleveland, Ohio USA • Phone: 216-529-3900; 800-822-4322 • Fax: 216-529-3975

11/96 2M

MBE ≈ Atomic Spray Painting